UNIVERSITÀ
DEGLI STUDI
FIRENZE

Doctoral Programme in Industrial Engineering

Dottorato di Ricerca in Ingegneria Industriale

XXXIII

Human-vehicle interaction in automated vehicles: the issue of carsickness

ING/IND-14

Doctoral Candidate

Cesare Certosini

Dean of the Doctoral Programme

Prof. Giampaolo Manfrida

Supervisors

Prof. Renzo Capitani

Dr. Claudio Annicchiarico

External referees

Prof. Alberto Bemporad

Prof. Filippo Cianetti

Years 2017/2020

to my dad
a mio padre

Summary

Motion Sickness (MS) is an issue of most transportation systems. Several countermeasures to this problem in cars are proposed in the literature, but most of them are qualitative, behavioural or involving complex chassis systems. Autonomous Driving (AD) can exacerbate the problem of MS due to the change from driver to passenger with the consequent loss of control over the vehicle With the growing interest in self-driven vehicles, the issue of MS may be so important as to undermine their benefits in terms of increased productivity; not addressing this issue may limit the users' acceptance reducing the safety and the environmental impact of autonomous vehicles.

In this thesis, the issue of carsickness is discussed, analysing the potential technologies to monitor MS in cars and discussing their feasibility.

After the analysis of the monitoring technologies, in the final part of the manuscript, the issue of reducing MS in cars is analysed, proposing optimal methods for carsickness reduction. To optimise the vehicle behaviour, two Model Predictive Control (MPC) problems are formulated to analyse the potential impact in different applications of optimal MS reduction techniques.

The first task is to find the optimal speed profile to travel on a given path while trading-off between minimal travel time and minimal Motion Sickness Incidence (MSI); in this part, several strategies are proposed and analysed comparing their performance. This novel methodology may be used in autonomous cars to create a reference velocity profile for lower control layers or, in human-driven ones, to advise the driver.

The second task applies only to autonomous vehicles, implementing the MS optimisation in the motion planning layer; a trajectory optimisation problem is solved using the best performing strategies of the optimal speed profile task.

The results show that optimising vehicle behaviour may significantly reduce the MSI, improving the user experience in cars; furthermore, the wider possibilities offered by autonomous cars allow for further reduction of MSI.

The optimal methodologies proposed and the strategies used are the main contribution of this doctoral thesis; the coherency of the results in the different cases analysed suggests that these strategies have a general validity for MS reduction.

In the conclusions chapter, the impact of these methods is discussed; possible ways of integrating MS monitoring technology into the proposed reduction techniques are analysed.

Preface

This research stemmed from my passion for cars and technology.

In years fast pacing automation of cars, technology enthusiasts are looking with high expectations to the potential of autonomous cars but how can we connect them with the rest of the population creating a positive emotional connection towards autonomous cars?

As a former often motion sick kid, in this research I tried to understand how to create more human-friendly autonomous cars by exploring the possibilities given by a greater level of automation.

I want to deeply thank all the people that supported me during this research, especially my supervisors that advised me during these years and the current and former doctoral students of my research group for sharing the endeavour of the doctoral years with me.

Contents

Summary v

Preface vii

1 Introduction 1
1.1 Reasearch question . . . 2
1.2 Thesis outline . . . 3

2 Motion Sickness 5
2.1 Signs and symptoms of motion sickness . . . 7
2.2 Motion sickness assessment methodology . . . 8
2.3 Theories of motion sickness . . . 8
2.4 Motion sickness countermeasures . . . 9
2.5 Motion sickness numerical models . . . 10
2.5.1 ISO 2631-1:1997 model . . . 10
2.5.2 Bos and Bles model . . . 11
2.5.3 UniPG SeMo model . . . 12
2.5.4 Kamiji et al. model . . . 12
2.6 The issue of carsickness . . . 12
2.6.1 In-vehicle motion sickness countermeasures . . . 15

3 Motion sickness monitoring 19
3.1 Heart Rate Variability . . . 20
3.1.1 Video based cardiac pulse estimation . . . 24
3.2 MSI estimation using numerical models . . . 25
3.3 Conclusion . . . 27

4 Optimal speed profile for carsickness reduction 29
4.1 Introduction . . . 29
4.1.1 Optimal approach to motion sickness reduction: a generalised quantitative approach . . . 29
4.2 Methods . . . 30
4.2.1 Road . . . 31
4.2.2 System dynamics . . . 31
4.2.3 Constraints . . . 33
4.2.4 Cost functions . . . 33
4.2.5 Composing the MPC problem . . . 35
4.2.6 Performance assessment . . . 35

4.3 Results . . . 36
4.4 Discussion . . . 39
4.5 Conclusion . . . 43

5 Trajectory optimisation for carsickness reduction 45
5.1 Introduction . . . 45
5.1.1 Research aim: MS reduction in motion planning . . . 46
5.2 Methods . . . 46
5.2.1 Road . . . 46
5.2.2 System dynamics . . . 47
5.2.3 Constraints . . . 48
5.2.4 Cost functions . . . 49
5.2.5 Composing the MPC problem . . . 50
5.2.6 Performance assessment . . . 50
5.3 Results . . . 50
5.4 Discussion . . . 55
5.5 Conclusion . . . 56

6 Conclusion 57

Bibliography 59

Acronyms 73

List of Figures

1.1 EU road fatalities: target and data [2] 2

2.1 MSI distribution at different frequencies and amplitudes 6
2.2 ISO 2631-1:1997 acceleration filter 10
2.3 Bos and Bles model 11
2.4 UniPG SeMo visual-vestibular interaction 12
2.5 Kamiji *et al.* model 13
2.6 augmented reality visual aids 16

3.1 cardiac pulse scheme 20
3.2 cardiac pulse resampling 21
3.3 tachogram resampling 21
3.4 RR histogram 22
3.5 HRV periodogram 22
3.6 Poincaré plot 23
3.7 resampled periodogram 25
3.8 head inclination effect on MSI 26

4.1 maximum MSI over total travel time for the analysed cost functions 37
4.2 comparison of three cost functions with similar maximum MSI . . . 38
4.3 comparison of three cost functions with similar travel time 38
4.4 Lomb-Scargle periodogram PSD estimate of three cost functions with similar travel time 40
4.5 velocity of three cost functions with similar travel time 41
4.6 MSI estimated using the ISO-2631-1:1997 approach 41
4.7 sensitivity analysis to different susceptibilities 42

5.1 track overview 47
5.2 comparison of proposed cost function – MSI evolution over time . . . 51
5.3 comparison of the different trajectories – turns 28 to 32 52
5.4 last lap velocity for the different cost functions 53
5.5 PSD of the last lap accelerations 54

List of Tables

4.1 conflict dynamics parameters value 32
4.2 MSI dynamics parameters value 32
4.3 common costs value 34
4.4 simulation results 36

5.1 costs used in the reported simulations 50
5.2 cost functions performance 51

Chapter 1

Introduction

Autonomous Driving (AD) is one of the main development fields of the automotive world. The human error is one of the main causes of road accidents [1], therefore, increased automation of cars will allow for safer roads and fewer road fatalities.

The European Union (EU) set the target for 2020 to reduce the road fatalities of 50% in a decade; however, the 14th Road Safety Performance Index Report [2] shows that this target is far from being reached: in 2019 the road fatalities have been reduced by 23.66% and, as shown in Fig. 1.1, from 2013 to 2019 the road fatalities have reduced of just 5.51%. This widening gap between the road fatalities and the EU 2020 target is a trend that goes on consistently from six years and it is extremely unlikely that the EU 2020 target will be reached.

Benefits of autonomous driving

To address this issue, AD may play a crucial role in road safety enhancement [3] but the benefits of AD are not limited to greater safety, but their use can also improve the mobility of certain parts of the population today struggling with their mobility needs [4]. AD helps also in stabilising the traffic flow [5], improving the traffic throughput of the roads and lower the environmental impact of the traffic due to the smoother velocities [6]; furthermore, AD should also favour the adoption of smart mobility approaches further improving the mobility in cities [7, 8] and it contributes alleviating the issue of parking [9]. Another expected impact of AD is the ability to use the time spent in the vehicle in different ways, not being focused anymore on the driving task; this should contribute to lower the value of travel time savings [10] since it is possible to do other tasks like working, interacting with other passengers, looking movies or resting up.

Autonomous driving: the issue of user acceptance

Studies show that some benefits of AD like traffic shockwave dampening require a small percentage of autonomous vehicles in the traffic mix, but other ones like a higher traffic throughput and a lower environmental impact require a higher adoption of autonomous cars [5].

For widespread adoption of AD the issue of user acceptance of this technology becomes critical: a survey by Bansal *et al.* shows how the users are most concerned of system failures, interaction with non-autonomous vehicles and the cost of

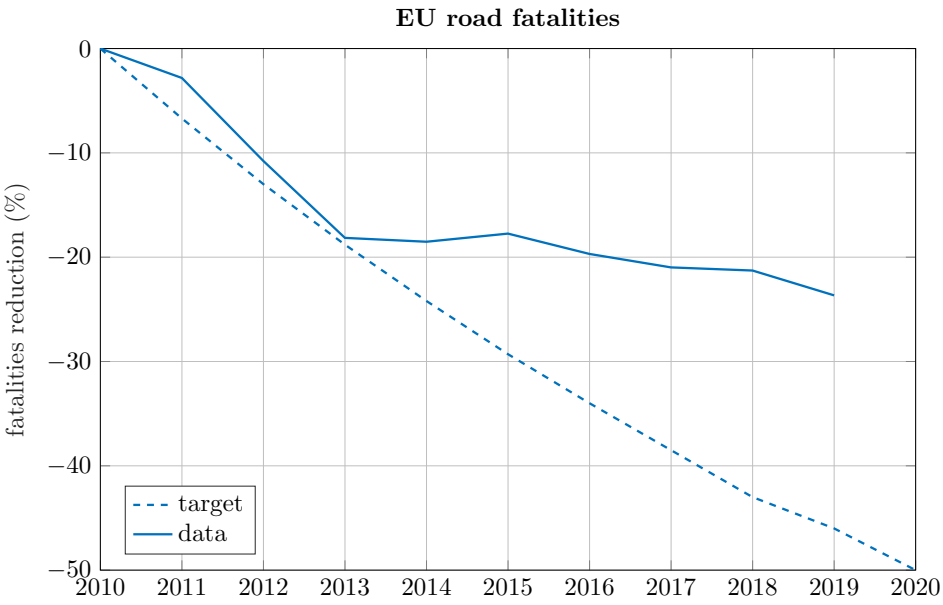

Figure 1.1: EU road fatalities: target and data [2]

autonomous cars; they also found that technology literate males, the ones who live in urban areas and higher-income peoples tend to be more in favour of AD. User acceptance also varies with cultural differences because there is variability between different nations [11–13].

With the increase of automation and the focus of the former driver now shifting away from the road ahead the issue of Motion Sickness (MS) will become even more important. In the literature are present several studies analysing how AD may lead to greater carsickness [14–16]. In a more provocative environment like autonomous cars, some of the claims that autonomous cars will increase the passengers' productivity may be at risk and some study are starting to describe the problem [17, 18].

If the issue of MS in cars is not addressed, it could affect user acceptance even limiting the other benefits of AD that require a large adoption, like the environmental ones and greater traffic throughput.

1.1 Reasearch question

Looking at the increasing importance of MS in the context of autonomous cars, it appears to be a need for addressing carsickness in automated cars.

To address this need, this research tries to answer the following question: *what are the possible ways to prevent the issue of MS in autonomous cars?*

This very general research question was then divided into two sub-question.

- Is it possible to monitor the onset of MS in passengers in a non-invasive way?
- And, more importantly, is it possible to control the automated vehicle in a way to prevent the issue of MS?

1.2 Thesis outline

In the following section, after explaining the research question and the motivation behind it, it is introduced the structure of the thesis which adheres to the research process followed to answer the research question

Motion sickness

In this chapter, the phenomenon of MS is described by reporting the results of an extensive literature review; due to the interdisciplinary nature of the issue of carsickness, MS is analysed starting from its symptoms, moving towards the main theories explaining why someone gets motion sick. After this, the countermeasures to this issue proposed in the literature are presented and discussed; later on, the numerical models of motion sickness are introduced. The last part of the chapter describes what are the main features of MS in cars and the proposed countermeasures.

Motion sickness monitoring

In this chapter is analysed the task of monitoring MS in cars; after discussing what are the symptoms measurable in cars without being too invasive, the feasibility of an Heart Rate Variability (HRV) analysis using cameras is analysed proving that a 60 Hz acquisition may still lead to reliable results. In the last part is analysed the effect of the head inclination in cars combining passengers' behaviour from the literature with acceleration data from Chapter 5 simulations; in this section, it is shown how the passengers' head pose plays a significant role in the evolution of MSI.

Optimal speed profile for carsickness reduction

In Chapter 4 a novel method to optimise the speed profile for MS reduction is presented. The optimisation is carried out formulating a Non-linear Model Predictive Control (NMPC) problem and comparing different strategies for MS reduction. First, the simulation environment and the road used for the simulations are introduced, then, vehicle model and the MS one are described; after that, the constraints are introduced as well as the definition of the different strategies within different cost function. Later on, the space transformation used in this chapter is introduced and the optimisation formulation is presented. At the end of the chapter, the simulations results are analysed discussing the different performances of the different cost functions.

Trajectory optimisation for carsickness reduction

By narrowing down the field to only autonomous vehicles, the MS reduction problem in Chapter 5 is formulated as a trajectory optimisation problem analysing the potential of introducing MS-related terms in the motion planning level. Like in the previous chapter, a NMPC problem is formulated trading off between minimal travel time and minimal MS. The introduction of the components of the simulation is similar to the previous chapter, therefore starting from the simulation environment, the road, the system dynamics, constraints, cost functions and the optimisation formulation; the cost functions compared in this chapter are the best performers of

the previous one, adapted to the different formulation of the problem. At the end of the chapter, the results are discussed analysing the potential benefits of using an autonomous vehicle, compared to a human-driven one, limited only to the optimal speed profile method of Chapter 4.

Conclusion

In the last chapter, the conclusions are discussed. These summarize the contributions presented in the previous chapters, highlighting how the research places itself respect to the state of the art; the impact of the research is analysed and possible evolutions of this research are proposed.

Chapter 2

Motion Sickness

MS has always been an issue of transportation systems since the dawn of humanity: the word *nausea* has its roots in the greek word $\nu\alpha\tilde{\upsilon}\varsigma$ which means *ship*, showing how this issue has always been present since the very first transportation systems.

MS is a state of disease caused by a provocative motion; several studies analysed what a provocative motion is. One of the fundamental studies is [19] by O'Hanlon and McCauley; in this study is analysed how the MSI, which is the percentage of people that would experience emesis, of subjects under vertical sinusoidal motion varies under different frequencies and different amplitudes. The results show that MS frequencies range from 0.01 Hz to 1 Hz with a peak at ≈0.16 Hz and the MSI increases with the increasing amplitude in a non-linear way. Results of this study are reported in Fig. 2.1.

MS has a wide coverage by the scientific community, and a summary of the several studies can be found in [20].

The main stimuli of MS are transportation systems and several studies report MS in sea ones [21–23], in road ones [24–27], in trains (especially analysing tilting ones) [28–31], in planes [32, 33] and even in space [34, 35]; every transportation system may lead to MS, but what is causing it?

Despite the obvious acceleration stimuli, MS can even be provoked by visual stimuli [36–39] and even auditory stimuli may induce it in the most sensitive subjects [40] or may help to mitigate it [41]; this suggests that MS is not just a susceptibility to some range of accelerations, but it is something more complex.

In recent years, the attention of the scientific community is focused on understanding the implications of incoherent environments, like simulators; in these environments, the vestibular information cannot match the visual and auditory ones due to the limited range of movement possible. Several studies cover the issue of simulator sickness [38, 42–44], showing how the incoherence between different sensorial inputs may increase the incidence of MS.

The chapter will analyse the different aspects of MS: it will start by describing the main symptoms related to MS, moving on to describing the main theories regarding how MS works; after that, the main countermeasures to MS are described. After understanding what MS is, how it is generated and what are the main strategies to prevent it, the chapter will cover the main numerical models describing the incidence of MS as a function of a given motion. The chapter will end by describing the specific issue of carsickness, how it relates to other types of MS and what strategies are proposed in the literature to prevent it.

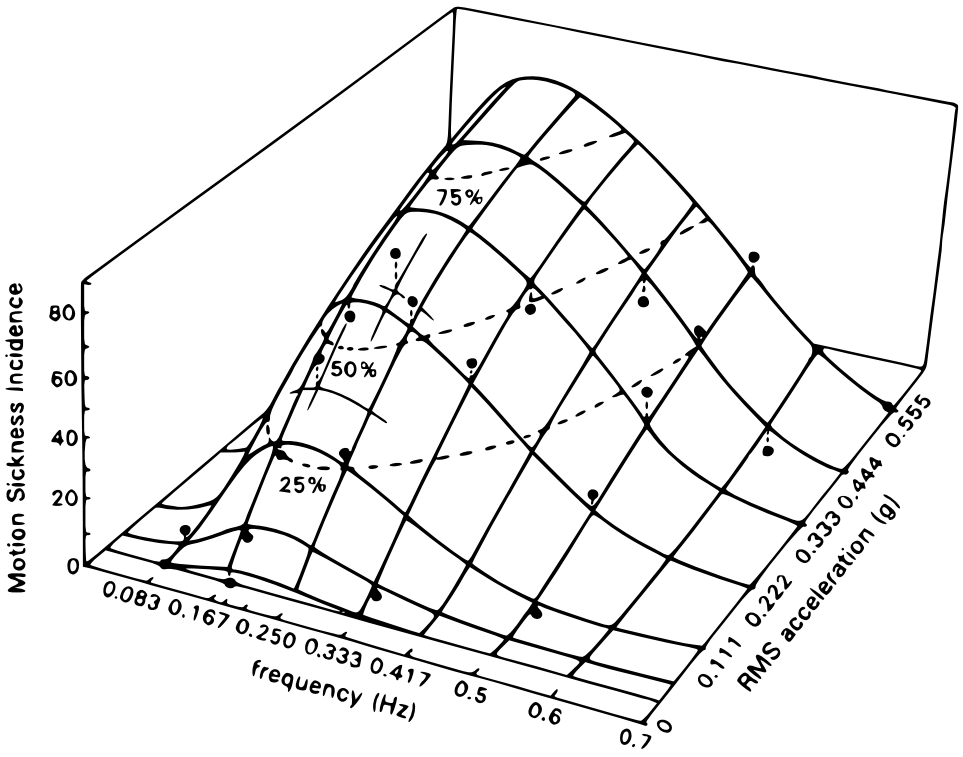

Figure 2.1: MSI distribution at different frequencies and amplitudes [19]

2.1 Signs and symptoms of motion sickness

The main symptom of MS is nausea, leading to emesis in the most extreme cases, but several other symptoms are related to MS: as reported in [45] and other research papers, the autonomic response typical of MS as a plethora of symptoms which are correlated with MS.

Gastric motility has the strongest correlation with MS [46–48] due to its vagal afferences. Nausea induced by MS is reflected as an increase in gastric activity; being, therefore, the most relevant physiological signal when discussing about MS, as it is closely related to the main symptom.

Another important correlation with MS is the HRV; due to cardiac sympathovagal interactions, several studies report a variation in HRV during provocative motion. The results, however, are quite incoherent and tend to report large interpersonal variability; the general trend related to MS is an increase sympathetic activity leading to an increase in low-frequency band (0.04 Hz to 0.15 Hz) and a decrease in the high-frequency one (0.15 Hz to 0.4 Hz), hence an increase in the LF/HF ratio. The studies [46, 49–53] tend to report one of the two variations or both, so the ratio may be a more general metric to identify MS, however other studies report contradictory results [42, 53] but this might be explained by counteracting strategies adopted by the users [53].

Hu *et al.* report a variaton in certain frequency bands related to MS [46].

Electro-Dermal Activity (EDA) has been studied in several papers [46, 54, 55]. Despite being a recognised symptom of MS, it lacks a strong correlation to MS because it is a response common to several psychological states; therefore, it might be prone to misinterpretation [55].

Analysing the temperature of the subjects under MS, it has been shown [56, 57] how during MS the body induces an hypotermic response leading to lower core temperature and vasodilatation.

Postural instability has been reported [58, 59] as a precursor of MS; however, it is also reported [60] how this is not a necessary condition for MS.

Temperature and humidity do not affect MS as reported in several studies [25, 61, 62]; odors [63] have no influence on MS, but MS can make unpleasant odors more unpleasant.

A particular symptom of MS is the sopite syndrome: in some subjects MS may lead to drowsiness and mood changes, as reported in several studies [33, 64, 65].

A major role in MS susceptibility is done by the previous experience of the subject; several susceptibility questionnaires [66] use subjects' MS history to estimate their susceptibility. MS is a phenomenon with a very big inter-personal variability, and the occurrence of symptoms heavily depends on the subject; for this reason, a history of susceptibility is an indicator of risk of suffering MS symptoms again when subject to provocative stimuli.

MS susceptibility is biased towards gender, race and age as several studies show: women tend to suffer more from MS [67, 68] and there is some evidence [68], in studies with mixed Chinese and caucasian volunteers, that race may also play a role; young children tend to be immune to MS, susceptibility begins approximately at age 6 with a peak around 9 years of age and decreases over teenage [25, 69, 70].

For deeper coverage of the argument the author remands to [20, 45].

2.2 Motion sickness assessment methodology

MS is a multifaceted phenomenon, and it is not straightforward to objectively determine when someone is motion sick; one of the most common methods is to interview the subjects with a given questionnaire.

The MS questionnaires can be divided in two categories:

- the MS susceptibility questionnaires, aiming to predict if a subject will be prone to MS before doing something that may be provocative,
- the MS assessment questionnaires, aiming to assess if the subject is motion sick while doing something that may be provocative.

The first group cover aspects like previous experience with transportation systems and previous experience of MS; the main questionnaires are the Motion Sickness History Questionnaire (MSHQ) from [71], the Motion Sickness Susceptibility Questionnaire (MSSQ) from [69] and the Motion Sickness Susceptibility Questionnaire Revised (MSSQR) from [66]. Since someone with an MS history tends to maintain a high susceptibility, the questionnaires give a higher score when more cases of MS are reported during the subject lifetime and tend to lower the score the more different types of transportation systems the subject has experienced.

The second type of questionnaire focuses on the development of symptoms and are useful to detect the evolution of MS during an experiment. They track different symptoms and give an aggregate score synthesising the actual MS state of the subject in a single numerical value. The main questionnaires of this group are the Pensacola Motion Sickness Questionnaire (MSQ) used in [72] and other papers, the Simulator Sickness Questionnaire (SSQ) [73] developed from the basis of the MSQ to assess simulator sickness, the Virtual-Reality Sickness Questionnaire (VRSQ) [74] used to assess MS in virtual environments. An important adaptation of the MSQ is the Motion Sickness Assessment Questionnaire (MSAQ) [49] from Gianaros *et al.*, deriving several subscores to give a better description of the evolution of the different symptoms. Förstberg *et al.* used the FACT Motion sickness questionnaire in [28] to assess MS in trains; this one is a simpler questionnaire consisting of just two general questions regarding the actual state of sickness and the one in the last 10 minutes.

2.3 Theories of motion sickness

The most important theory explaining MS is the sensory conflict theory; the human brain receives information about the motion in several ways: the vestibular, visual, kinaesthetic and auditory inputs are fused in the brain to understand how the body is moving; information about previous experiences is used in the fusion process. When the inputs are not coherent, MS can be triggered.

Several explanations of this phenomenon are proposed in the literature; the most important one is presented by Treisman in [75] and is largely accepted in the community [76]. The theory explains the emetic response of MS as if the brain interprets the sensory conflict as a sign of poisoning triggering the emetic reflex; the theory is elegantly explained in [77]: *All situations which provoke motion sickness are characterised by a condition in which the sensed vertical as determined on the basis of integrated information from the eyes, the vestibular system and the*

nonvestibular proprioceptors is at variance with the subjective vertical as expected from previous experience.

Another important theory is the one of postural instability presented by Riccio and Stoffregen in [78] and discussed in [79].

To explain the *why* of MS is difficult; in [80] there is some scepticism about taking one of the theories as an established truth due to the practical difficulties of proving why MS works the way it is.

2.4 Motion sickness countermeasures

The main suggested countermeasure to MS is habituation. As discussed in the sensory conflict theory, the several inputs are fused with a sort of internal model built on previous experience; therefore, training the subject to the new inputs of a new environment reduces the occurrence of MS. Training programs are used by the military and for space crews training [81–83]; they reduce susceptibility without side effects, but are very time consuming, hence, are not suitable for large-scale use. MS habituation is very effective, but it is also stimuli-specific: in [84] is reported how car-sickness resistance may not translate into sea-sickness one; however, some form of general habituation is reported in the literature [85, 86].

Although of little relevance for this thesis, pharmacological countermeasures are partially effective but have several side effects [20, 45]; moreover, the development in this field is not particularly encouraging [45].

Galvanic Vestibular Stimulation (GVS) has an influence on MS [87] and can be used for astronauts training [88] or to mimic the vestibular perception in simulators [89] to reduce sensory conflict in those incoherent environments.

Experimental evidences [90, 91] show that controlled breathing can improve MS resistance.

Another behavioural countermeasure against MS is to align the head with the Gravito-Inertial Acceleration (GIA) [92–94]; since gravity is aligned with the head while standing, humans tend to be more resistant to vertical accelerations compared to horizontal ones.

A study [95] shows that motion in the frontal direction is less provocative if the subject is supine compared to when the subject is upright, suggesting that if the movement aligns with the gravity tends to be less provocative; this is different from the findings of [92] because in [95] is analysed if the movement aligns with the gravity with the same orientation between motion and vestibular system, while in [92] is analysed if the vestibular system aligns with the sum of motion and gravity. This study may be of little relevance in transportation systems because motion orientation with respect to the environment can not be changed, so the orientation between motion and gravity is not a manipulatable variable.

Moving from the theory of postural instability, restraining head and body movements might be helpful to prevent MS [96]; however, this may be incompatible with comfort requirements, and it may be a hindrance in carrying out tasks.

Several countermeasures can be elaborated by exploiting the sensory conflict theory. In cars, it is a common experience that drivers tend to be immune to MS [97]; this is due to anticipatory information that drivers have for being in control of the vehicle, allowing to better predict with his internal model what accelerations will perceive [77, 98, 99]. Feeding information about the environment lowers the

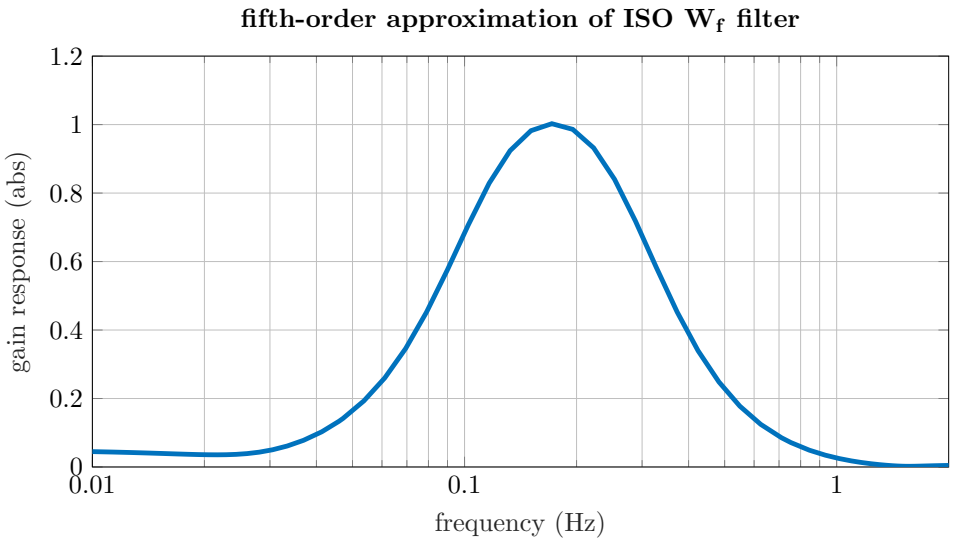

Figure 2.2: fifth-order approximation pf ISO 2631-1:1997 W_f acceleration filter [104]

risk of MS [24], while performing tasks involving fixation of objects moving with the subject (therefore having a static visual field) improve the incidence of MS [27].

A study shows how a stroboscopic illumination helps to prevent MS in military helicopters by preventing retinal slip [100].

2.5 Motion sickness numerical models

Numerical models describing MS tend to estimate the MSI from the subject's motion; their main inputs are the translational accelerations of the head (modelling the otolith perception); however, some models also use the rotational velocities perceived by the semicircular canals.

The fundamental experimental study, which almost every model refers to, is [19]; in this study, the MSI is a function of the amplitude of the sinusoidal vertical motion of this test and its frequency; the results of this campaign are shown in Fig. 2.1.

The models can be divided into two main categories:

- the models related to the standard ISO 2631-1:1997 [101]
- the models derived from the Bos and Bles model [102]

Ancillary models modelling specific parts of the sensory conflict mechanism are also present, like the one presented by Telban and Cardullo modelling the visual-vestibular interaction [103].

2.5.1 ISO 2631-1:1997 model

The ISO model is derived from the work of Lawther and Griffin presented in [105]; it works by filtering the accelerations with a filter fitted over data from several

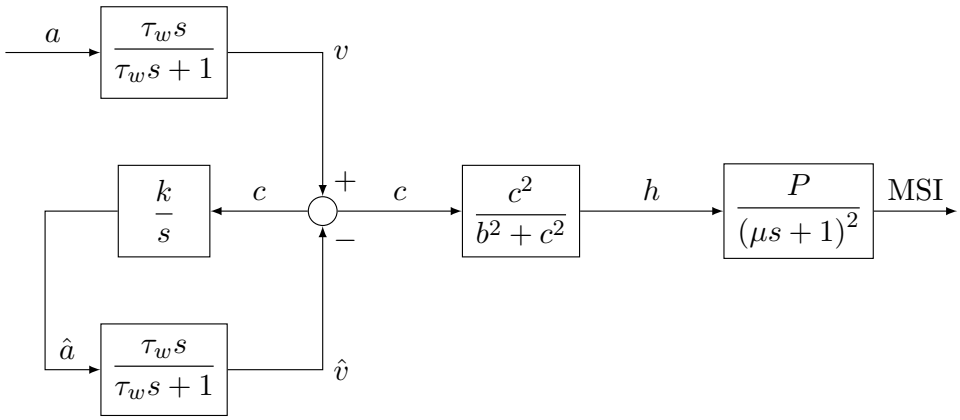

Figure 2.3: model presented by Bos and Bles in [102]

laboratory and sea surveys. Low-order approximation of this filter is presented in [104] and the fifth-order one is shown in Fig. 2.2. The filtered acceleration is weighted according to the axis (1.4 for the horizontal axis and 1 for the vertical one), and the Motion Sickness Dose Value (MSDV) is computed as in Eq. (2.1).

$$\mathrm{MSDV}_T = \sqrt{\int_0^T a_w^2(t)\,\mathrm{d}t} \tag{2.1}$$

MSI is derived from MSDV as in Eq. (2.2).

$$\mathrm{MSI} = \frac{\mathrm{MSDV}}{3} \tag{2.2}$$

The main issue with this model is that MSI cannot decrease over time; because of this, this model is not very good in estimating MSI over long and varying environments like road travels, while it may be good for relative comparison of the provocativeness of different motions. Studies [106] report poor fitting of the literature data [107].

2.5.2 Bos and Bles model

This model, presented by Bos and Bles in [102], mathematically describes the perception of the vertical direction using a lowpass filter; the perception is compared with the expected vertical from an internal model to compute the sensorial conflict. The conflict is non-linearly weighted using a Hill function to get the instantaneous disturbance, mimicking the non-linear relation found in the literature. The instantaneous disturbance is fed in a second-order transfer function to compute the MSI.

The use of a second-order transfer function allows modelling the decrease of MSI when the instantaneous disturbance decreases.

The model is shown in Fig. 2.3.

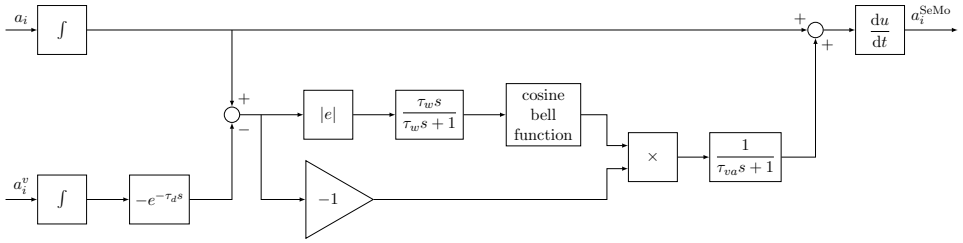

Figure 2.4: UniPG SeMo visual-vestibular interaction [106], adapted from [103]

2.5.3 UniPG SeMo model

This model, presented in [106], is a three-dimensional extension of the Bos and Bles model; the base UniPG model has no significant differences to the Bos and Bles model. The UniPG SeMo model integrates also the visual-vestibular interaction from [103], with minimal modification; the scheme of the visual-vestibular interaction is reported in Fig. 2.4. The acceleration perceived from the vestibular system a_i is corrected with a term based on the difference between a_i and the acceleration perceived from the visual system a_i^v; the resulting acceleration a_i^{SeMo} is fed into the UniPG model to compute the conflict along the i$^{\text{th}}$ axis.

The three-dimensional extension is done by computing the conflict for each direction, weighting vertical and horizontal ones: referring to Fig. 2.3, $k = 1.4$ is used for the horizontal directions and $k = 1$ for the vertical one. The three conflicts are joint in the Hill function by using the square of the magnitude of the conflict vector ($c^2 = c_x^2 + c_y^2 + c_z^2$); the instantaneous disturbance is fed into the MSI dynamics as in [102].

This model has been compared to the ISO 2631-1:1997 one in [106] by fitting literature data [107], analyse how this model fits better the literature data and can model the recovery after the motion. A survey of MS in trains is presented in [29] comparing the model estimation with the survey data: given all the uncertainties in the comparison between the survey and the numerical data, the results show an agreement between the subjective and objective data.

2.5.4 Kamiji et al. model

The model presented by Kamiji *et al.* in [108] is an evolution of the Bos and Bles one modelling the semicircular canals; the semicircular canals sense the rotational velocities of the head, allowing a better description of the sensory conflict dynamics. The model showed in Fig. 2.5, clearly resembles the Bos and Bles one, featuring a similar topology; the conflict between sensed and expected vertical is fed into the Hill function similarly to the Bos and Bles and the UniPG SeMo model.

The model is compared to experimental data available in the literature showing a good correlation.

2.6 The issue of carsickness

Carsickness is a common version of MS; it is well-known by the general public due to the wide use of road vehicles. Several studies analysed this phenomenon; among the main ones, [24–26] from Turner and Griffin analysed 3256 passengers of 56 UK

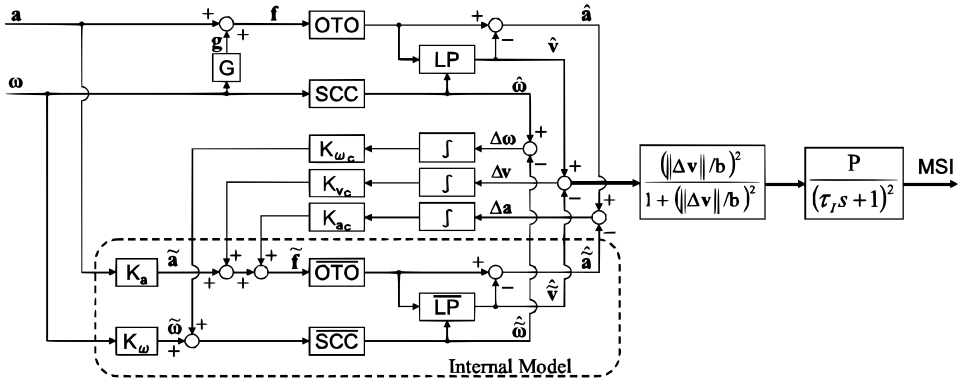

Figure 2.5: Kamiji *et al.* model [108]

bus or coach journeys. The authors reported how MS varies compare to different aspects; the main findings are:

- 28.4% of passengers reported feelings of illness,
- 12.8% reported nausea,
- 1.7% reported vomiting during coach travel,
- there is a strong dependency with previous cases of MS,
- passengers more experienced in bus travelling are affected less than less experienced ones,
- higher accelerations tend to be more provocative,
- the drivers driving with higher accelerations tend to induce more MS,
- the cross-country roads have higher records of MS, and, also, are the ones with the highest lateral accelerations,
- MS increases towards the rear of the buses, where the forward vision is more restricted,
- women tend to suffer more than men,
- older persons tend to suffer less than younger ones,
- no variability is reported between different bus models.

The findings suggest, similarly to the rest of MS versions, that there is a strong interpersonal variability with a strong influence of motion habituation. Moreover, the driving style and the type of road influence greatly the reported MS, this opens the possibility to adapt the driving style to more provocative roads and susceptible passengers to reduce the MSI.

As with the other types of MS, lower accelerations create less conflict; to avoid conflict it is also important to have a clear view of the road ahead to anticipate with the visual information the vestibular stimuli.

Other authors report evidence that being focused on reading [27], or just not being able to look-ahead [94], can increase MS severity.

The need for information about the upcoming motion can be relevant in the use of modern infotainment systems, with bigger screens allowing for more interaction with the passengers.

Another important factor in cars is passengers head movement: Zikovitz and Harris in [109] compared driver and passengers head tilting behaviour. They found that the driver tends to lean the head inside the corner; however, the correlation with the lateral acceleration is not very strong. They suggest that the driver tends to lean the head according to the curvature of the road ahead, anticipating the upcoming motion; passengers, instead, tend to lean the head towards the outer of the curve, passively responding to the lateral acceleration.

Several authors argue if this behaviour may have a relation with the higher susceptibility of the passengers compared to the driver one; Wada *et al.* analysed in [92] the MSI using different postural behaviours.

Using the Kamiji *et al.* model to estimate the MSI evolution, they simulated different head reactions to the lateral acceleration:

1. compliant condition: the head leans outwards like the passengers
2. vertical condition: no head leaning
3. resistance condition: opposite leaning than the compliant condition
4. GIA condition: the head vertical is aligned with the GIA

The results show that leaning the head inwards drastically reduces the MSI with a minimum value for the GIA condition; leaning outwards, as most passengers do, is the worse scenario between the analysed ones. The main issue of the GIA condition is that it requires very large tilting angles with 20° required for just 0.36 g of lateral acceleration.

The same research group carried out an experimental campaign [94] to analyse the same phenomenon: during a series of slalom runs they analysed the passengers leaning the head inward and outwards validating the numerical results of [92].

The same passengers were also divided into two groups depending on having their eyes open or closed: the passengers with the closed eyes had higher sickness ratings than the ones looking at the road ahead, according to the previous findings in the literature [24].

The passengers with the closed eyes reported consistently higher sickness ratings than the ones looking ahead, independently of the head leaning behaviour: this suggests how the vestibular-visual mismatch, and the lack of preparation for the vestibular stimuli, play a bigger role than the head movements.

In autonomous vehicles, there is a shift from driver to passenger, reducing the controllability of the former driver on the vehicle. This change exacerbates the sensory conflict; for this reason, the issue of MS is even bigger than in human-driven cars [16].

Several studies analysed this issue and tried to give a clear picture of the potential implications between MS and AD; the findings suggest that self-driving cars require special attention to the issue of MS, and this should be addressed since the vehicle design phase [15]. Failing to do so may impact heavily on the benefits of autonomous vehicles, by impeding the passengers to focus on productivity tasks while being in a

car [17]; if the discomfort of automated vehicles due to MS will be too big, it may even affect the user acceptance of this technology, limiting the benefits in terms of road safety and traffic flow.

2.6.1 In-vehicle motion sickness countermeasures

Limiting MS in cars involves exploiting the several aspects of MS.

The simplest and most effective method, as with any kind of MS, is to habituate to the motion; however, this can be done only in specific cases (like people using the same bus to go to work), and it requires significantamount of time to get used to the provocative environment; therefore, it is not a comprehensive solution to the issue of carsickness.

Other useful methods are the behavioural approaches: they have the big drawback of requiring a proactive mindset by the user, but they can help in reducing the MSI without having negative side effects, just like the user habituation.

The two behavioural approaches are:

- actively looking the road ahead
- aligning the head with the GIA

The first method is rather easy to do; however, it cannot be applied in every situation: if the passenger has to read something because he is working or the field of view is covered (like in the rear seats if the front seats are too high or too bulky), the passenger cannot take advantage of this countermeasure; evidence of the high effectiveness of this method are reported in [24, 94].

The second method has been analysed by Wada *et al.* in several studies, both numerically [92, 110, 111] and experimentally [93, 94], as described in the previous section; instructing the passengers to align the head properly may decrease the MSI in vehicles.

Results similar to the head tilting approach can be obtained by using an active chassis system tilting the body of the vehicle or the passengers' seats; tilting trains are studied in the literature [28, 31, 112] and are reported to reduce the MSI if the control system has a very low delay. A similar approach can be thought for cars, and has been proposed by Sugiura *et al.* in [111].

Another work presenting an active chassis system is [113] by DiZio *et al.*: they presented a system filtering the vertical inputs from the road in the frequencies of MS; they claim that this active system can be useful in preventing MS.

Moving from active chassis systems to design guidelines, Bohrmann *et al.* show experimental results suggesting that a reclined seated position may reduce the MSI; this is in accordance on what found in laboratory by Golding *et al.* in [95].

To reduce the sensory conflict, aside the looking forward approach discussed before, the focus of the scientific community is posed on the maximisation of the information fed to the passengers. Kuiper *et al.* suggest in [115] to design the infotainment system placing the displays at the same height of the windows, to view the road ahead with the peripherical view even when the passenger is focused on a display.

Salter *et al.* suggest avoiding rearward facing seats [116]; they show evidence of greater provocativeness compared to the forward-oriented ones. Diels *et al.* in [15] suggest to maximise the area of the windows, to reduce the obstruction of the A-pillars, to lower the shoulder line and to raise the seats to allow the passengers

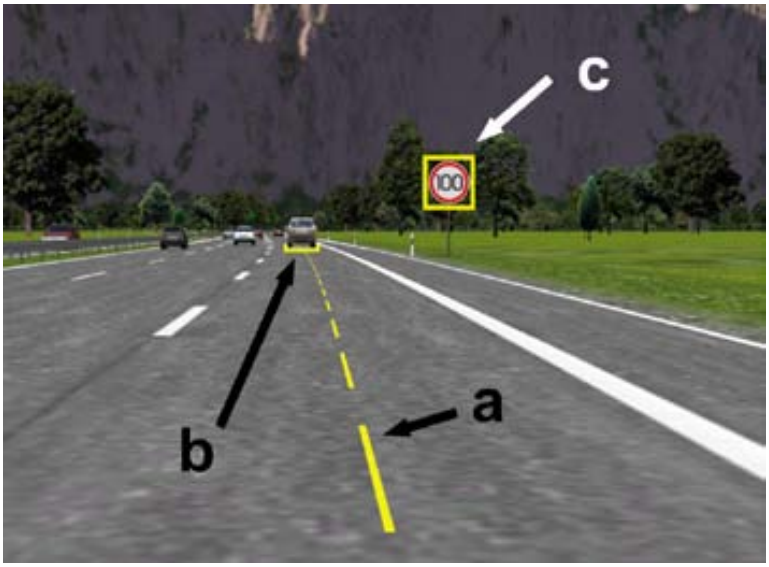

Figure 2.6: Augmented reality visual aids in automated vehicles to reduce MSI [119]

to look out easily; it has to be noted how such requirements may conflict with the safety ones.

The papers described before tends to ease as much as possible the collection of information by the passenger; however, feeding information to the passengers is an active research topic. Karjanto *et al.* show [117] how putting some lights next to an infotainment display signalling the vehicle motion reduce the MSI allowing for greater comfort when enjoying come content on a display.

Similarly to Karjanto *et al.*, Meschtscherjakov *et al.* propose to add some visual clues about the vehicle motion on a smartphone screen to counteract MS [118]; a similar system can be added on the car infotainment displays with similar benefits using the information coming from the vehicle sensors.

Feenstra *et al.* show in [120] that adding information to the environment about the vehicle predicted movement, by using techniques like augmented reality, can greatly reduce the MSI. This work, done in a flight simulator, can be used in cars by using an Head-Up Display (HUD) similar to the one proposed in [119] and showed in Fig. 2.6. Such system can be used only in automated vehicles, because in human-driven one, a stable vehicle movement prediction may become an impossible task; moreover, it is questionable how to scale such device in a multi-seated vehicle.

The approach proposed in [41] is easier to implement in autonomous vehicles: feeding audio information to the passengers can mitigate MS; however, using a visual clue like in [120] would provide a greater reduction.

MS is one of the main concerns about the big change in user experience in autonomous vehicles; however, increased automation also offers new possibilities to limit this problem. A novel approach to the issue of carsickness in AD has appeared in the scientific community in the last year: the idea is to exploit the flexibility in controlling the vehicle motion given by the fact that the vehicle is no longer controlled by a human, but it is controlled by an algorithm; if this algorithm takes into account the issue of MS, the severity of MS in autonomous vehicles may be

addressed by exploiting the specific possibilities given by this technology.

In [121] the authors controlled the lateral dynamics of a car by using a Stanley controller [122] and correcting the input steering wheel angle to limit the lateral acceleration; this correction is done using a fuzzy-PID where the gains are computed solving an optimisation problem receiving as input the head roll angle and its roll velocity.

In [123] a scheduled Linear Quadratic Regulator (LQR) where the feedback gain optimisation takes into account the lateral acceleration filtered using the W_k and W_d filters from the ISO 2631-1:1997 standard; it should be noted that the authors used the filters intended for the whole body vibration assessment when, instead, they should have been used the W_f filter. They analysed a double lane change manoeuvre and assessed how the MSDV of their control is lower than a traditional scheduled LQR; however methodological question may be issued due to the use of the incorrect filters: if they have not used the best-suited filter in the computation of the feedback gains it should be supposed that the same approach is used for the computation of the MSDV, the standard instead uses the W_f filter to compute a_w in Eq. (2.1)

The most interesting paper, regarding vehicle control for MS reduction, optimise the speed profile over a given path [124]. The vehicle is simplified as a point-mass model constrained on the spline representing the road with an acceleration circle modelling the available grip (it is not specified the maximum acceleration); a Model Predictive Control (MPC) problem is formulated computing the optimal speed profile along the path. The optimisation cost function is made summing two terms: the first one maximise the longitudinal speed (since the vehicle is constrained on a spline, maximising the speed means to minimise the travel time), the other one minimise the illness rating that is proportional to the MSDV as defined in ISO 2631-1:1997. The roads used to run the simulations consists in a road less than $<$300 m long, with a left and right turn at constant curvature; the three roads used differ by the curvature of the turns.

The results show that by varying the weighting cost a trade-off between minimum time and minimum MSDV can be carried out, tuning the control according to the user's needs.

Chapter 3

Motion sickness monitoring

Once presented the characteristics of MS, it is important to analyse how this phenomenon can be tracked in a car. As discussed in Section 2.1, the main symptoms of MS are very invasive to measure; therefore, symptoms like gastric activity and internal temperature have to be discarded.

The role of previous experience may be accounted for setting how the monitor or reduction system should be invasive so that the passengers may adjust it based on their susceptibility; this can take into account even the gender and racial bias of MS.

The detection of the sopite syndrome may be done by monitoring the passengers' drowsiness; today, several methods have been developed to monitor the driver's drowsiness [125], the methods based on eye-tracking may be used to monitor the passengers one. In a vehicle, using Electro-OculoGraphy (EOG) for eye-tracking is not feasible; for this reason, PERCLOS and blinking frequency measures can only be done using cameras, like in [126].

Since monitoring EDA would require the use of electrodes on the passengers, this method can be considered too invasive.

Postural instability can be monitored by estimating the head acceleration using cameras; the same estimation can be fed into numerical models to give a prediction of the current MSI of the passengers. The accuracy of numerical models can be significantly improved using camera-based head acceleration estimation and pose estimation. These models can be used feeding the vehicle acceleration; however, they should use the actual head acceleration to give a personalised MSI estimation for each passenger. Moreover, the head inclination plays a big role in MS, as shown in [92]. At the end of this chapter, the potential of the head inclination effect on MSI is analysed by using the UniPG model [106] and the passengers head inclination behaviour reported in [109].

A very interesting measure is the HRV: with the growth of wearable devices, a vehicle can use information coming from a wearable device estimating HRV with the use of photoplethysmography. In this chapter, the issue of HRV estimation is analysed, and it is analysed how this challenge can be addressed in cars.

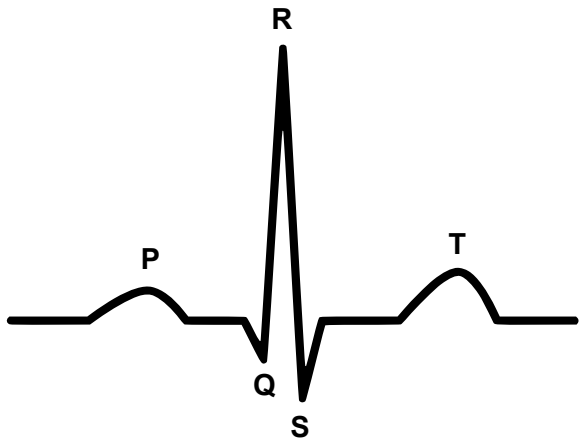

Figure 3.1: cardiac pulse schematics with labelled salient points [127]

3.1 Heart Rate Variability

HRV is a measure of the oscillation in the interval between consecutive heartbeats (the Inter-Beat Intervals (IBI)); the usual measure of the HRV analyse variation in the normal RR intervals (also called NN intervals), which are the intervals between two consecutive R peaks (shown in Fig. 3.1) corrected to eliminate artefacts.

To extract HRV, the first step is to create the tachogram: starting from the cardiac pulse acquisition (e.g. the blue line of Fig. 3.2), the peaks are identified and filtered to remove artefacts by using filtering techniques available in the literature [128–131], creating the normalised RR intervals, also called NN intervals.

Once the RR intervals are normalised, the tachogram is constructed by plotting the beat-to-beat interval against the time; this creates a plot (e.g. the blue line of Fig. 3.3) whit an uneven spacing of the data points because the spacing on the x-axis varies according to the value of the y-axis.

The NN intervals can be analysed using several methods to extract information about the HRV [132]; these methods can be categorised in:

- time-domain methods
- frequency-domain methods
- non-linear methods

The time-domain methods rely on the analysis of the distribution of the IBI: a typical approach is to evaluate the standard deviation of the distribution. The normal fitting of the IBI distribution is shown in Fig. 3.4.

The frequency-domain methods consist of analysing the power of the high-frequency (from 0.15 Hz to 0.4 Hz) and low-frequency (from 0.04 Hz to 0.15 Hz) bands of the tachogram Power Spectral Density (PSD); very-low-frequency are not of interest in the analysis of MS related HRV. The bands of interest of the Fig. 3.3 tachogram, in its Lomb-Scargle periodogram, are shown in Fig. 3.5.

The non-linear methods consist of several different methods for analysing the tachogram data; however, there is no defined standard on how and when to use them. One of the methods is the Poincarè plot described by [133] and with practical

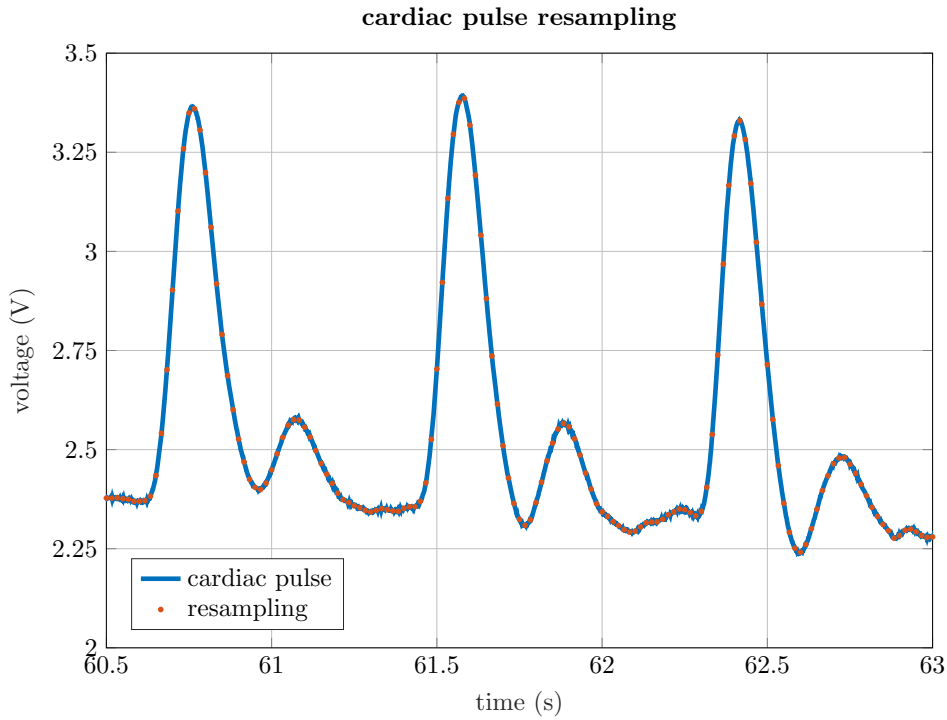

Figure 3.2: cardiac pulse acquisition – 1 kHz data and 60 Hz resampling comparison

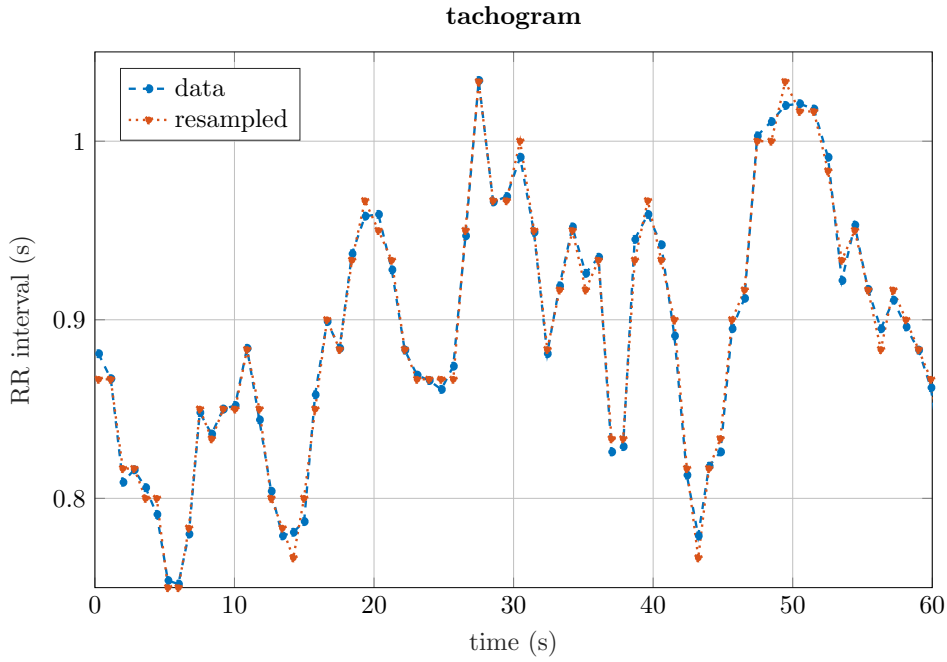

Figure 3.3: tachogram – 1 kHz data and 60 Hz resampling comparison

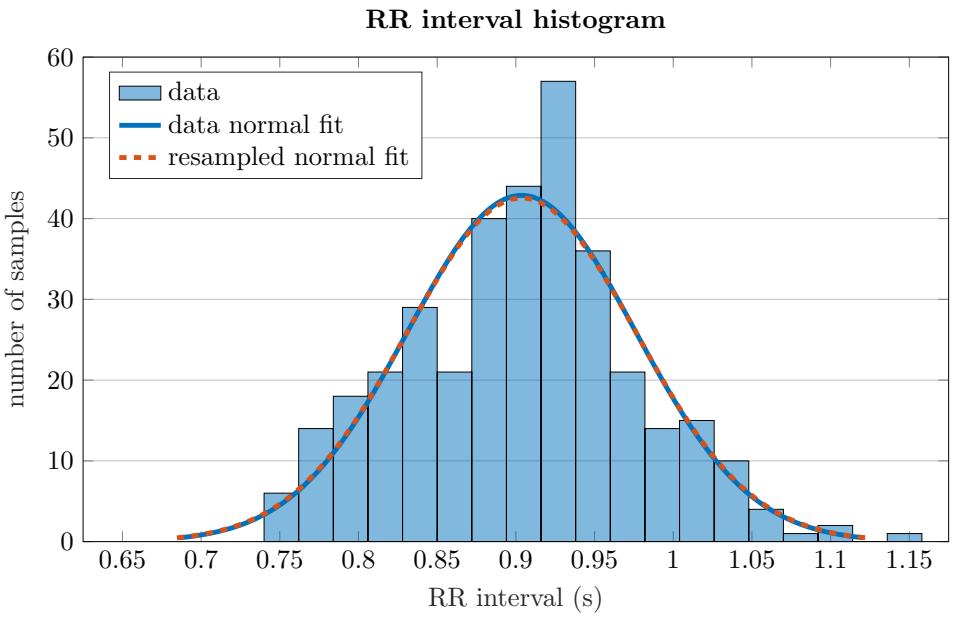

Figure 3.4: RR histogram – normal fitting of the RR intervals histogram

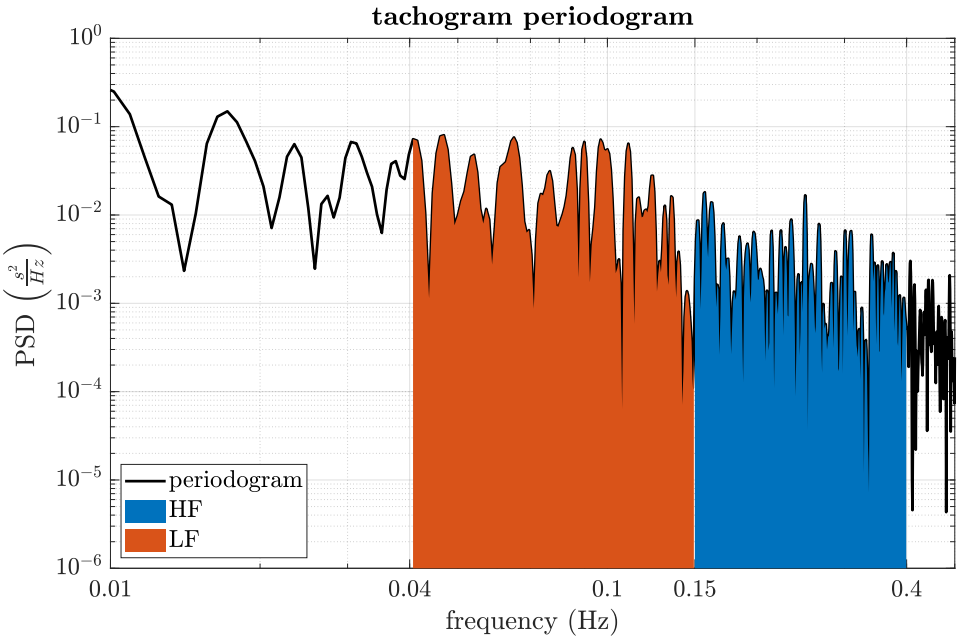

Figure 3.5: HRV periodogram – with the LF component analysed in orange and the HF one in blue

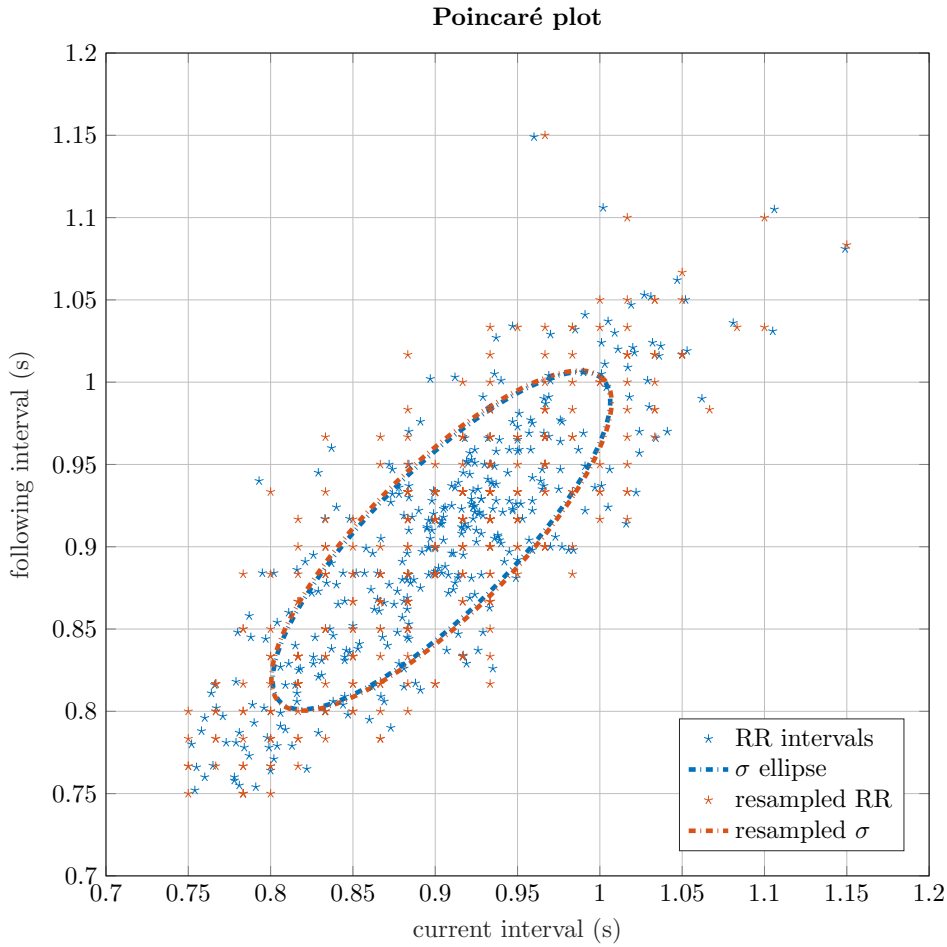

Figure 3.6: Poincaré plot – comparison between 1 kHz raw data and 60 Hz resampling

consideration in [134]: by plotting the current interval and the following one, a 45° rotated ellipse can be fitted on the data, where the semi-axes are the standard deviation of the data on the ±45° directions; the −45° semi-axis is the peak-to-peak variability, while the 45° one is a description of the general variance of the IBI. An example of the Poincaré plot with the standard deviation ellipse is shown in Fig. 3.6.

3.1.1 Video based cardiac pulse estimation

A relevant new technology in cardiac-related data acquisition is the video-based cardiac pulse estimation: Poh *et al.* presented in [135, 136] a method to extract the heart rate from a video by using the Viola and Jones method [137] to identify the face Region Of Interest (ROI) and performing Indipendent Component Analysis (ICA) [138, 139] on the pixel RGB data of the ROI. The proposed method has been proven very effective in the estimation of the heart rate data in laboratory condition [136, 140–142], however, its main limitation is in the robustness of the Viola and Jones algorithm for face detection.

By using Artificial Neural Networks (ANN) for detection, the robustness of the data can be dramatically increased [143]; a possible approach may be to detect the facial landmarks and to select the region within the landmarks. An example of the facial landmark capabilities can be found in [144]. Another improvement available using a facial landmark approach is to use just the cheeks and the nose to limit artefacts due to blinking and speaking.

Guo *et al.* in [143] show how when upgrading from ICA to Indipendent Vector Analysis (IVA) [145, 146] the accuracy further improves.

In [143] show how combining the facial landmark approach (using as a subregion of the face) and using IVA to extract the cardiac pulse can significantly improve the heart rate estimation.

However, despite some demonstration in [135] using Viola and Jones and ICA, there isn't a study demonstrating the feasibility of HRV estimation using a camera, ANN and IVA.

Video HRV estimation: feasibility analysis

The purpose of this chapter is to study the feasibility of estimating the HRV signal using a video. To do that, a cardiac pulse is acquired using a *Pulse Sensor* photoplethysmograph connected to a National Instruments USB-6002 DAQ with a 1 kHz sampling rate.

The acquisition is then downsampled at 60 Hz (Fig. 3.2) to mimic a camera sampling rate and the HRV of the original data and the resampled one are analysed using time-domain, frequency-domain and Poincaré plot-based methods. The sampling rate of the acquisition for HRV should be ≥100 Hz and optimally >250 Hz; to understand if the downsampling due to a video estimation of the cardiac pulse may impede HRV analysis using a camera, further analysis is due. For this reason, in this section, the downsampled data are compared to the original one to demonstrate the feasibility of camera-based HRV estimation.

The tachogram of the two signals are fairly coherent, as shown in Fig. 3.3, despite in Fig. 3.2 the sampling of the R peaks is quite low in the resampled data.

The normal fitting of the resampled data is close to the original one, as shown in Fig. 3.4, therefore it should not affect any time-domain analysis.

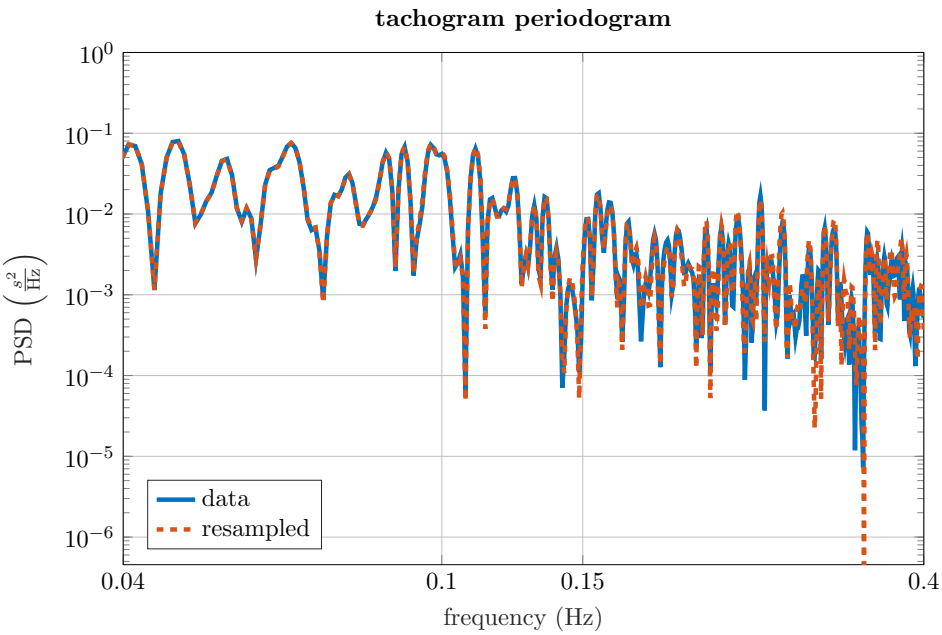

Figure 3.7: resampled periodogram – comparison between 1 kHz raw data and 60 Hz resampling

The periodogram of the resampled data is close to the original one, as shown in Fig. 3.7, therefore it should not affect any frequency-domain analysis.

As shown in Fig. 3.6, the ellipse of the resampled data of the Poincaré plot is close to one of the original data; despite the resampling of the data is visible in the scatter plot of the IBI. The similarity of the ellipses should guarantee that Poincaré plot analysis of the resampled data will preserve the information of the original one.

Downsampled data gave similar results to the original one, demonstrating that camera-based HRV analysis is possible; further research is due to implement the techniques proposed in this section and to experimentally assess the results in a car. A camera-based video system using ANN and IVA to analyse the HRV of the passengers may be used to monitor MS in cars using physiological feedback from the passengers; more research is due to demonstraate its effectiveness in the wild, but in this section has been shown how the camera downsampling may not prevent HRV per se.

3.2 MSI estimation using numerical models

Measuring physiological signals to detect the MS onset may help to control the issue of carsickness; however, having a system monitoring the current MSI may contribute to preventing MS in a more progressive way. The most straightforward way to track the MSI is to use numerical models of MS estimating the MSI using the vehicle acceleration.

Despite doing that may be a good way to estimate the MSI, something more can be done to take into account the interpersonal variability and the impact of the

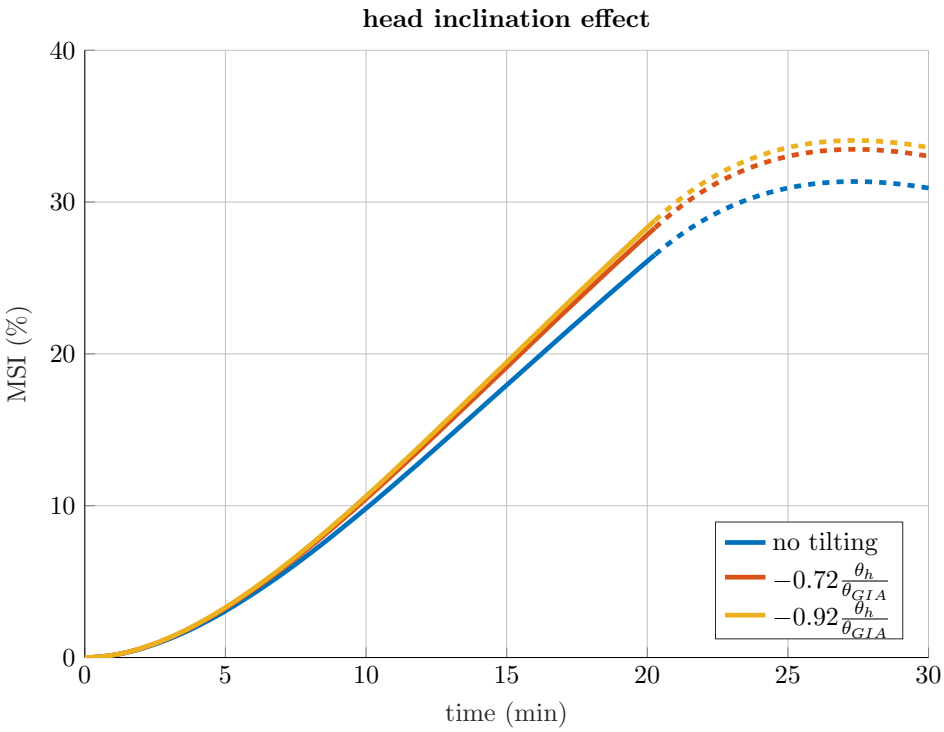

Figure 3.8: head inclination effect on MSI – comparison between 0°, −0.72° and −0.92° of head inclination per degree of GIA inclination

passengers' behaviour like in tilting the head [92] or looking at the road ahead [94].

According to the studies of Zikovitz and Harris, the passengers tend to recline their head outwards proportionally to the lateral acceleration [109]; the gain between head inclination and lateral acceleration is different if the passenger is looking ahead (−0.72° per degree of GIA inclination) or keeps the eyes closed (−0.92° per degree of GIA inclination).

To understand how much the head rotation can affect the MSI, the gains reported by Zikovitz and Harris are used to rotate the vehicle acceleration; the rotated accelerations are used to compute the MSI using the UniPG model, which is compared with the non-rotated one.

The accelerations used are the results of the minimum time strategy of the trajectory optimisation problem presented in Section 5.3.

By rotating the acceleration field the MSI increases from $\approx 31\%$ to $\approx 34\%$, therefore it is quite considerable for a short simulation like the one used; Wada *et al.* also show in their work [92] how this effect has a significant impact on the MSI.

To monitor the head inclination behaviour, a 3D head tracking system like the one proposed in [147] can be used. These systems may feed the head acceleration and rotation velocities to numerical models like the UniPG or the Kamiji *et al.* one.

Head video tracking can also be used to estimate the sway relative to the car to monitor the subject's postural instability, which, according to [79], may identify the onset of MS.

3.3 Conclusion

In this chapter, the physiological signals suitable to monitor MS in vehicles are analysed and discussed. In cars, it is critical to have contactless monitoring of MS; for this purpose, the related physiological signals have to be selected on the feasibility of their contactless estimate. In this chapter, the main ones are analysed, and it is shown how the HRV can be the most feasible physiological signal thanks to the possible camera-based estimate.

To demonstrate the feasibility of a camera-based HRV estimate, an HRV analysis of a 1 kHz sampled photoplethysmograph has been done using time-domain, frequency-domain and Poincaré plot-based methods and the results are compared to the same acquisition downsampled at 60 Hz.

The results show that although the downsampling affects the peak detection (as visible in Figs. 3.2 and 3.6 on page 21 and on page 23), the HRV-related quantities of the various methods are not affected, allowing for a HRV estimate using a camera.

In the second part of the chapter, the effect of the head inclination on the MSI has been analysed; using head inclination patterns from the literature on the results of Chapter 5 on page 45 shows that the head pose has an important effect on the MSI; this suggests how head pose estimation techniques like [148] can improve the MSI tracking when done using MS numerical models.

Chapter 4

Optimal speed profile for carsickness reduction

4.1 Introduction

MS monitoring can be a powerful tool to control the issue of carsickness; however, the main issue of the monitoring technologies proposed is that they detect the MS during its onset, so it is difficult to prevent it. The modelling of MS provides useful information to the passengers and can be helpful to the driver in human-driven cars, but how can we take advantage of this information in autonomous vehicles?

The idea behind this chapter is to explore the feasibility of exploiting the numerical models presented in Section 2.5 to optimally trade-off between the minimal travel time, which requires high accelerations, and the minimal MSI, which requires the lowest accelerations possible.

4.1.1 Optimal approach to motion sickness reduction: a generalised quantitative approach

A numerical model of MS is needed to assess the effectiveness of this trade-off; moreover, although these models are needed to assess the performance of the MS reduction strategy implemented in this chapter, are they necessary to get a lower MSI?

Now that the reasons, the current knowledge and the general idea about this research are introduced, the goal of this research can be clearly defined: finding an optimal way to travel on a path trading off minimum travel time and minimal MS. Such technique, if proven to be effective, may be used to plan the speed profile of an autonomous vehicle, to suggest an optimal speed profile to a human driver or to plan a more comfortable speed profile for bus line services or train services. Such a solution can be combined with the other countermeasures available in the literature to further reduce MS. Its main benefits compared to the one already available in the literature are:

- it does not rely on passenger behaviour,
- it can be applied to already designed vehicles,

- it does not require complex active systems on the vehicle,
- it does not require complex Human-Machine Interface (HMI) in the vehicles.

Using the numerical model to assess the performance of the proposed algorithm allows to quantitatively evaluate the results just on an average estimate of the population. In an actual implementation of this technique, the fact of assessing the performance against an estimate of the general population may be overcome by allowing the users to tune how important the MS reduction part of the optimisation is. Using a multi-objective cost function, like the ones presented in this chapter, leads to a straightforward implementation of the trade-off tuning by varying the MS related cost in the cost function.

4.2 Methods

A simulation approach is used to compare different strategies to optimise the speed profile on a given path. The results are analysed to understand if the modelling of MS dynamics is the best approach to the trade-off between minimum travel time and MS reduction or some strategy may be effective without the explicit modelling of MS.

The problem is implemented as a series of NMPC problems representing the vehicle moving on the path through a series of sequential optimisations. This approach allows us to solve a series of smaller optimisation problems instead of a single huge one; moreover, this technique is easily implementable in a real-world scenario with limited lookahead and subject to change when the passenger desires to change his route. The NMPC has been implemented in MATLAB and solved using the *fmincon* solver. Perfect knowledge of the system is assumed; therefore, the first predicted step of the optimisation is the actual step used in the next optimisation loop. As shown in [19], MS frequencies range from 0.01 Hz to 1 Hz, therefore the simulation step size has to be set to at least 2 Hz to get a proper description of MS dynamics. To correctly model such frequencies, each optimisation step size should be 0.5 s. As will be later explained, the optimisation is not time-integrated, but space integrated, and the velocity varies during the optimisation routine; for this reason, the space step size is defined as the distance covered in 0.5 s at the initial velocity of the optimisation routine. This approach leads to a different step size between low-velocity sharp turns and high-speed straights, preventing an inefficient low step size due to the space transformation. The predicted horizon is 12 simulation steps long and the input of each step is a manipulated variable; therefore, at the k^{th} step the actual state x_k is known and the optimisation predicts 12 state steps (from $\tilde{x}_{k+1|k}$ to $\tilde{x}_{k+12|k}$) and 12 input steps (from $\tilde{u}_{k|k}$ to $\tilde{u}_{k+11|k}$).

At the end of the optimisation routine, the system is updated by assigning the first predicted states as the new actual state and the first predicted input as the new actual input:

$$\begin{cases} x_{k+1} = \tilde{x}_{k+1|k} \\ u_k = \tilde{u}_{k|k} \end{cases} \tag{4.1}$$

4.2.1 Road

A test path is represented using a two-dimensional spline: the road used in this paper is a 120 km part of an Italian motorway. Since automated driving will first be used in motorways, it has been chosen to use this scenario for the simulations; however, the proposed approach is not limited to this scenario. The spline is created from an internet map service, transforming the latitude-longitudinal waypoints in North-East-Down coordinates leading to a flat x-y description of the test path. Several map services were compared, but different waypoints density between map services does not lead to significant changes in the resulting spline. The vertical contribution of the road is neglected simplifying the formulation to a two-dimensional problem. The path can be divided into two main sections: a first winding section characterised by a mountain crossing and a final straighter section; the first section is long nearly twice the later one.

4.2.2 System dynamics

Vehicle model

A vehicle model is needed to get the vehicle acceleration. Since the focus is not about a specific type of vehicle but the optimisation of MS on a given path, and since MS is characterised by very low frequencies compared to the chassis dynamics ones, the simplest vehicle model is adopted: a point-mass model, which is fast to compute while being general for different vehicles.

The vehicle is constrained on the road spline, without any displacement in the normal direction; therefore, the input of the model is only the longitudinal jerk j_t. The lateral acceleration a_n is computed from the longitudinal velocity v_t and the path curvature ρ.

$$\begin{cases} \dot{v}_t = a_t \\ \dot{a}_t = j_t \end{cases} \tag{4.2}$$

$$a_n = \rho v_t^2 \tag{4.3}$$

Motion sickness model

Motion sickness is modelled using the UniPG model [106]; the MS model is computed for every strategy tested to get the evolution of the MS incidence along the path, even when it is not used in the cost function.

The use of a Bos and Bles derived model allows for the modelling of the MSI decrease when the road tends to be less provocative, which can be useful in very long travels with long straight sections.

The model, as shown in Section 2.5 is composed of three main part:

1. the conflict generation from the perceived acceleration
2. the non-linear weighting of the conflicts in the different directions into an instantaneous disturbance
3. the MSI generation from the instantaneous disturbance

Table 4.1: conflict dynamics parameters value

α_1	α_2	α_3	γ_1	γ_2
-3.33	-4.18	-2.33	2.36	3.93

Table 4.2: MSI dynamics parameters value

π_1	π_2	σ
$-2.22e^{-3}$	$-1.23e^{-6}$	$1.05e^{-4}$

The first part is defined in the original model as a series of transfer functions and a feedback loop; in this work, it is computed an equivalent transfer function formulation, and it has been transformed in a state-space representation described in Eq. (4.4), using the parameters listed in Table 4.1. The state-space of the i^{th} direction has three states $c_{i_{1:3}}$, a single input a_i which is the acceleration in that direction and it outputs the conflict in that direction c_i.

$$\begin{cases} \dot{c}_{i_1} = \alpha_1 c_{i_1} + \alpha_2 c_{i_2} + \alpha_3 c_{i_3} + a_i \\ \dot{c}_{i_2} = c_{i_1} \\ \dot{c}_{i_3} = c_{i_2} \end{cases} \qquad \text{where} \qquad c_i = \gamma_1 c_{i_1} + \gamma_2 c_{i_2} \tag{4.4}$$

Eq. (4.4) is used once for each direction; it is used for the longitudinal direction using a_t as input, and for the lateral one using a_n (as defined in Eq. (4.3)) as input.

In the second part, the non-linear weighting transforms the conflicts (c_t, c_n) in the different directions into a single instantaneous disturbance h using the Hill function in Eq. (4.5).

$$h = \frac{c_t^2 + c_n^2}{b^2 + c_t^2 + c_n^2} \qquad \text{where} \qquad b = 0.7 \tag{4.5}$$

In the third part, the transfer function is again transformed in a state-space notation, shown in Eq. (4.6), with the parameters listed in Table 4.2. This part is a state-space with two states $c_{ms_{1:2}}$, with the instantaneous disturbance h as input and the MSI as output.

$$\begin{cases} \dot{c}_{ms_1} = \pi_1 c_{ms_1} + \pi_2 c_{ms_2} + h \\ \dot{c}_{ms_2} = c_{ms_1} \end{cases} \qquad \text{where} \qquad \text{MSI} = \sigma c_{ms_2} \tag{4.6}$$

Space transformation

To avoid issues due to the constantly changing curvature during optimisation, the problem has been space transformed like in [149–152]; so, it is space integrated instead of time-integrated. This allows for a fixed curvature during the optimisation,

even if it leads to a non-linear vehicle model; since the MS model is non-linear in itself, non-linearity in the vehicle model was considered of minor concern, and it was preferred to a changing curvature during the optimisation routine.

The transformation modifies the state dynamics equations as in Eq. (4.7), where x' is the space derivative.

$$x' = \frac{\dot{x}}{v_t} \tag{4.7}$$

4.2.3 Constraints

To be more representative of a touring driving, the vehicle acceleration has been constrained to be less than 0.3 g.

The jerk is also constrained to generate a smooth acceleration profile within $\pm 3\,\mathrm{m/s^3}$.

The longitudinal velocity is constrained to be between 60 km/h to 120 km/h.

$$\begin{cases} a_t^2 + \rho v_t^2 - (0.3\,\mathrm{g})^2 \leq 0 \\ -3\,\mathrm{m/s^3} \leq j_t \leq 3\,\mathrm{m/s^3} \\ 60\,\mathrm{km/h} \leq v_t \leq 120\,\mathrm{km/h} \end{cases} \tag{4.8}$$

4.2.4 Cost functions

The analysed strategies trading-off between MS and travel time are implemented into several cost functions of the NMPC problem; their results are compared to understand which is the most effective in preventing MS while keeping minimal travel time.

The cost functions compared in this chapter are:

1. minimum time cost function,
2. minimum longitudinal jerk cost function,
3. minimum acceleration cost function,
4. minimum instantaneous disturbance cost function,
5. adaptive minimum instantaneous disturbance cost function.

The strategies analysed are a reference strategy, two strategies without a MS numerical model and two using a MS numerical model.

Minimum time strategy

Each cost function has a term to minimise the travel time and a very small cost on the longitudinal jerk since it is the system input; these common terms are the only parts composing the minimum time cost function. This cost function is used as a reference to evaluate the performance of the other cost functions.

Since the vehicle is constrained on a spline, minimising the travel time or maximising the vehicle speed are exactly equivalent; therefore, the minimum travel time cost function is:

Table 4.3: common costs value

C_t	C_u
50	$1e^{-3}$

$$J_k = \sum_{n=1}^{12} C_t \frac{1}{\tilde{v}_{t_{k+n|k}}} + C_u \tilde{j}^2_{t_{k+n-1|k}} \tag{4.9}$$

Where J_k is the cost at the k^{th} time step, C_t is the minimum time cost, C_u is the input cost and $\tilde{v}_{t_{k+n|k}}$ is the longitudinal velocity v_t at the $k+n^{th}$ step predicted at the k^{th} step. The value of the common costs (C_t, C_u) is constant between the several simulations analysed, and their value is reported in Table 4.3.

Minimum longitudinal jerk strategy

Since the jerk has long been used as a comfort-related metric [153, 154], the first cost function analysed tries to minimise the longitudinal jerk, by replacing the small C_u cost with an equivalent C_j. Therefore, the minimum jerk cost function shown in Eq. (4.10) is almost the same of Eq. (4.9).

$$J_k = \sum_{n=1}^{12} C_t \frac{1}{\tilde{v}_{t_{k+n|k}}} + C_j \tilde{j}^2_{t_{k+n|k}} \tag{4.10}$$

Minimum acceleration strategy

MS models use often the acceleration as their input, as in [19, 102, 105, 106]; so, it is interesting to understand if reducing the input without modelling its dynamics may be sufficient to reduce the incidence of the discomfort.

A simple reduction of the maximum acceleration allowed without modifying the cost function has been proven in [155] to be ineffective.

For this reason, the second model-less strategy tries to reduce the acceleration using a cost C_a on the vehicle acceleration.

$$J_k = \sum_{n=1}^{12} C_t \frac{1}{\tilde{v}_{t_{k+n|k}}} + C_u \tilde{j}^2_{t_{k+n-1|k}} + C_a \left(\tilde{a}^2_{t_{k+n|k}} + \left(\rho_k \tilde{v}^2_{t_{k+n|k}} \right)^2 \right) \tag{4.11}$$

Minimum MS strategy

The first model-based strategy uses a cost C_{MS} on the instantaneous disturbance h to reduce the MSI; since the Hill function limits its value between 0 and 1, there is no need to use its squared value. The cost function is shown in Eq. (4.12).

$$J_k = \sum_{n=1}^{12} C_t \frac{1}{\tilde{v}_{t_{k+n|k}}} + C_u \tilde{j}^2_{t_{k+n-1|k}} + C_{MS} \tilde{h}_{k+n|k} \tag{4.12}$$

Adaptive minimum MS strategy

MS is a phenomenon with slow dynamics and takes several minutes to have a high MSI; for this reason it may not be very efficient to limit the vehicle speed in short paths where the MSI is very low. This strategy is shown in Eq. (4.13).

$$J_k = \sum_{n=1}^{12} C_t \frac{1}{\tilde{v}_{t_{k+n|k}}} + C_u \tilde{j}^2_{t_{k+n-1|k}} + C_{MS} \widetilde{\mathrm{MSI}}_{k+n|k} \tilde{h}_{k+n|k} \tag{4.13}$$

This approach, compared to the previous one, is capable of adapting itself to the road characteristics: if the road is too short to be relevant for MS, a low *MSI* will allow a speed profile closer to the minimum time one, when the path is long, it will slow down the vehicle during winding sections. Due to this characteristic, the more advanced model has been named *adaptive MS model*.

4.2.5 Composing the MPC problem

The MPC problem is built by assembling the parts explained in the previous paragraphs; the system dynamics are composed by the vehicle dynamics, two blocks (one for each direction) of the conflict dynamics equations, a Hill function and the MSI dynamics equations. Composing the system dynamics to the constraints and cost functions described above leads to the formulation described in Eq. (4.14).

$$\begin{gathered} \min_{x,u} J_k \\ \\ \text{subject to:} \\ x_0 = x(0) \\ x_{k+1} = f\left(x_k, u_k\right) \\ a_t^2 + \rho v_t^2 - \left(0.3\,\mathrm{g}\right)^2 \leq 0 \\ -3\,\mathrm{m/s^3} \leq j_t \leq 3\,\mathrm{m/s^3} \\ 60\,\mathrm{km/h} \leq v_t \leq 120\,\mathrm{km/h} \end{gathered} \tag{4.14}$$

4.2.6 Performance assessment

The performance of each cost function is assessed using the UniPG model comparing the maximum MSI obtained along the path against the travel time; the lower the time with the same maximum MSI, the more efficient the cost function is.

Robustness with respect to different MS numerical models

The main part of the analysis focuses on how the different strategies reduce MS, evaluating the MSI with the UniPG model. This method uses one of the most advanced MS numerical models, both for the performance assessment and (in the strategies using a MS numerical model) for the optimisation. To understand whether the best performing strategies are reducing MS or are exploiting a numerical loophole, the results are also evaluated using the ISO 2631-1:1997 model: coherent results would confirm the robustness of the results with respect to the metric used; to do that the fifth-order filter proposed in [104] is used to approximate the ISO filter.

Table 4.4: simulation results

Cost function	Cost	MSI max (%)	Travel Time (min)
min time		31.7	58 min 26 s
min jerk	$C_j = 40$	43.7	1 h 7 min 31 s
min jerk	$C_j = 200$	41.3	1 h 6 min 43 s
min jerk	$C_j = 1500$	38.6	1 h 7 min 55 s
min acceleration	$C_a = 10$	21.3	1 h 11 min 0 s
min acceleration	$C_a = 15$	19.8	1 h 14 min 42 s
min MS	$C_{MS} = 75$	23.1	1 h 9 min 22 s
min MS	$C_{MS} = 140$	21.0	1 h 11 min 32 s
min MS	$C_{MS} = 170$	21.5	1 h 11 min 49 s
min MS	$C_{MS} = 200$	22.2	1 h 11 min 44 s
adaptive min MS	$C_{MS} = 24$	20.6	1 h 9 min 3 s
adaptive min MS	$C_{MS} = 25$	20.0	1 h 9 min 48 s
adaptive min MS	$C_{MS} = 27$	18.3	1 h 11 min 37 s
adaptive min MS	$C_{MS} = 30$	17.7	1 h 12 min 9 s
adaptive min MS	$C_{MS} = 40$	14.8	1 h 16 min 20 s

Different susceptibility across the population — sensitivity analysis

After the performance analysis of the different strategies, it is interesting to analyse how the strategies would perform in populations with different susceptibilities. According to the results available in the literature, Bos and Bles derived models replicate the experimental literature results with good accuracy, but they work by modelling the average sensitivity of the population. How would these model more susceptible (or more resistant) parts of the population? In that case, how the optimisation strategies should adapt to model this variability?

The most straightforward approach is to increase the MS-related cost, and the results of this are shown in the main part of the analysis; however, it can be argued that in a more susceptible population, a higher MSI should be expected. To model this alternative approach, after the main results, a sensitivity analysis has been carried out by simulating the most relevant strategies in a standard, a highly susceptible and a lower susceptible population. To model the different susceptibilities, the b gain of the non-linear conflict weighting of Eq. (4.5) is set to 0.6 for the highly susceptible population and 0.8 for the less susceptible one.

This analysis is meant to understand whether the optimal methods behave consistently when varying the susceptibility; however, an experimental investigation is needed to understand if varying the non-linear weight is appropriate when modelling different susceptibilities.

4.3 Results

The results are summarised in Fig. 4.1: the shorter the travel time and the lower the MSI the better; for a list of cost values for the various runs see Table 4.4.

The base model is, obviously, the fastest, with a travel time of ≈58 min; the maximum MSI of ≈ 32% indicates quite a severe risk of emesis.

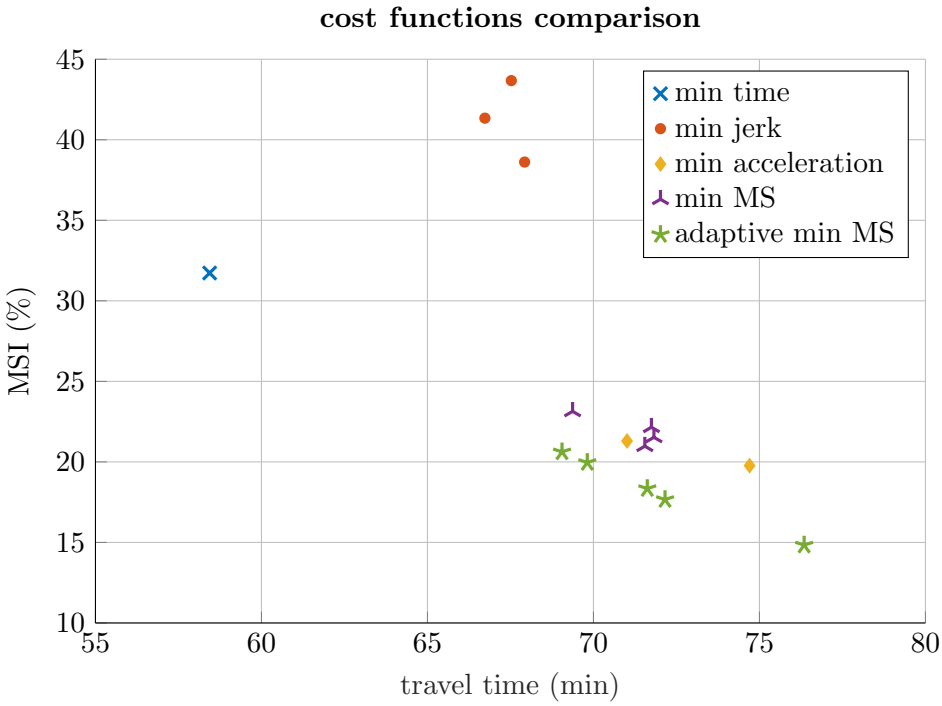

Figure 4.1: maximum MSI over total travel time for the analysed cost functions

Despite its usage for comfort assessment, using the jerk to reduce MS is ineffective. The jerk cost function has the highest MSI, and it is also quite slow.

The acceleration cost function proves to be very effective; it provides a significant reduction of MSI over the minimum time strategy, and a variation of C_a affects the trade-off between minimum time and low MSI.

An interesting result is the simple MS cost function one: just optimising h in the optimisation is effective indeed, but it is not more effective than just trying to reduce the acceleration. For the same MSI peak value, the travel time is usually higher than the acceleration run, therefore such technique is less efficient than the acceleration strategy. For values of C_{MS} in the $140 - 170 - 200$ range, the model has almost the same MSI and the same travel time, possibly due to some numerical issues for this cost function.

The adaptive MS cost function is the best performer of all those tested. This cost function provides the lowest MSI among all and is substantially the most efficient between the three effective ones in reducing the MSI; comparing the runs with $C_a = 10$, $C_{MS} = 140$ and $C_{MS} = 24$ in Fig. 4.2, the adaptive cost functions is faster by over two minutes compared to the others. When looking for lower MSI values, the difference in time between the adaptive cost function and the acceleration cost function increases dramatically: for an MSI of $\approx 21\%$ the difference between the two cost functions is $\approx$2 min, while for a MSI of 20% the difference in time rise to $\approx$5 min.

When looking at a travel time of $\approx$71 min, the adaptive cost function reduces the maximum MSI to $\approx 18\%$ instead of the $\approx 21\%$ of the acceleration and simple MS cost functions.

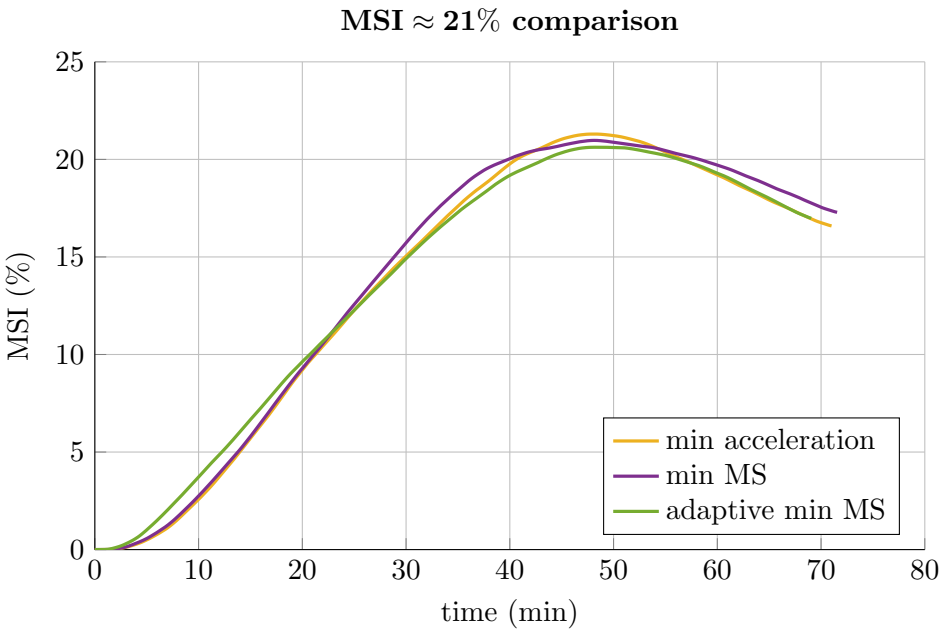

Figure 4.2: comparison of three cost functions with similar maximum MSI

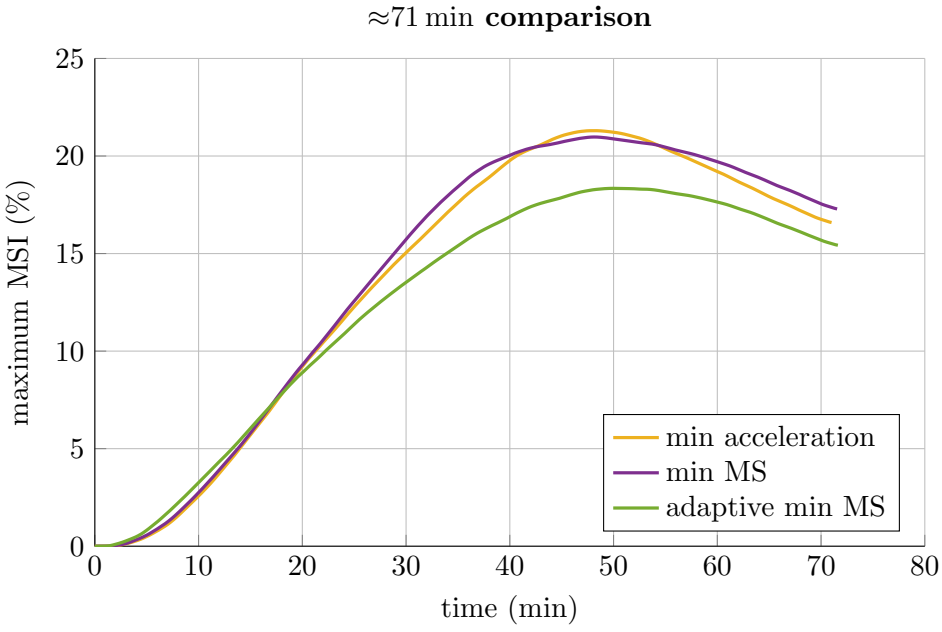

Figure 4.3: comparison of three cost functions with similar travel time

Looking at the evolution of the MSI over time for runs with similar maximum MSI (Fig. 4.2), the difference between the adaptive cost function and the simpler MS one is interesting: at the beginning, the lower overall MS cost ($C_{MS}MSI$) give higher MSI values, however, for higher MSI, the adaptation of the more complex cost function pays off, keeping the MSI below the simpler cost function.

When comparing runs of similar duration (Fig. 4.3), it is clear how the adaptive cost function outperforms the others. To analyse how this cost function outperforms the others, in Fig. 4.4 the Lomb-Scargle periodogram has been computed to estimate the PSD of the accelerations of the simulations shown in Fig. 4.3. It is shown how the longitudinal accelerations a_t have a similar spectral composition, but the lateral accelerations a_n differ quite significantly, coherently to the MSI difference between the three cost functions.

The use of the adaptive minimum MS strategy allows for a better behaviour in straighter sections like from 75 min to 85 min of Fig. 4.5, where the adaptive strategy is faster than the minimum acceleration one despite leading to a lower MSI.

4.4 Discussion

The results show that the presented optimisation is effective in reducing passengers discomfort. Introducing additional terms within the motion planning algorithm to increase passengers comfort is effective even without actively modelling the MS dynamics, as for the minimum acceleration cost function. The best strategy for a simple implementation of an MS reduction algorithm might be the minimum acceleration one. For the best performance in terms of MS reduction and minimal time, however, an adaptive minimum MS strategy is needed. The simple minimum MS strategy is not more effective than the minimum acceleration one, not justifying the additional burden of optimising the MS dynamics.

The MSI data can be used as feedback to the passengers: when using the minimum acceleration strategy, the MSI needs to be computed as a separate task, while when using the adaptive minimum MS strategy, the information is already available because it is part of the optimisation.

It is interesting to notice how the minimum acceleration strategy is effective while a simple reduction of the maximum acceleration is not, as shown in [155].

The PSD analysis showed that the main difference between the different cost functions with similar travel time is in the lateral dynamics as studied in the experiments of Wada *et al.* in [93].

Given the innate variability from person to person in the phenomenon of MS, the numerical models are not accurate in modelling the single passenger. For this reason, it is interesting to compare the obtained results between the proposed cost functions using the ISO 2631:1997 approach to understand if the results are consistent and can be taken as a general improvement of comfort. The results showed in Fig. 4.6 are consistent with the ones in Fig. 4.3. The adaptive cost function is the most effective approach and the most efficient, and the simple MS and acceleration cost functions have similar performance; it is interesting to notice the adaptation phase in the first minutes of the adaptive cost function.

Such coherency suggests that the proposed strategies offer an improvement in terms of MSI, so the gain is not just a numerical trick due to using the same algorithm in optimisation and performance assessment.

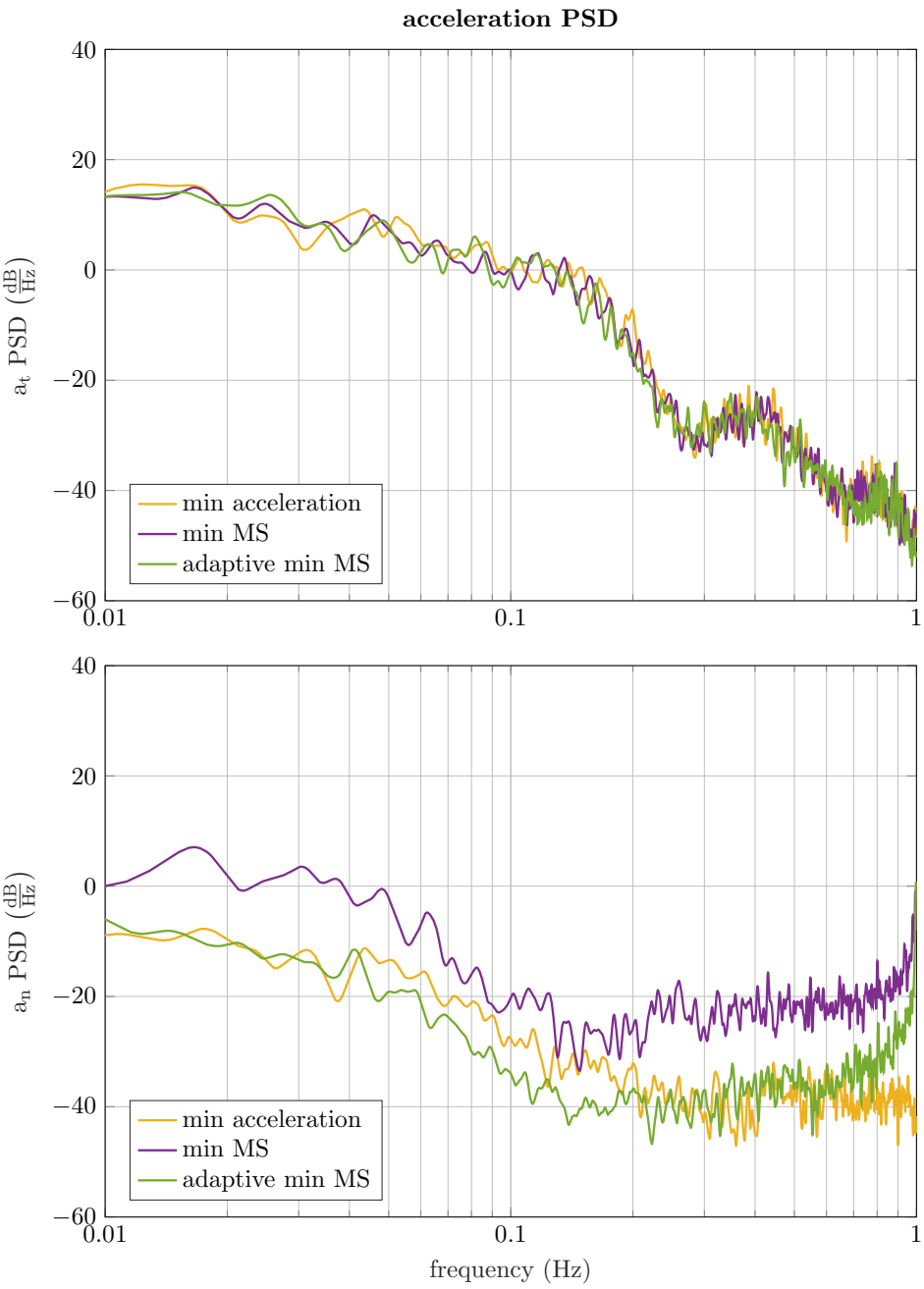

Figure 4.4: Lomb-Scargle periodogram PSD estimate of three cost functions with similar travel time

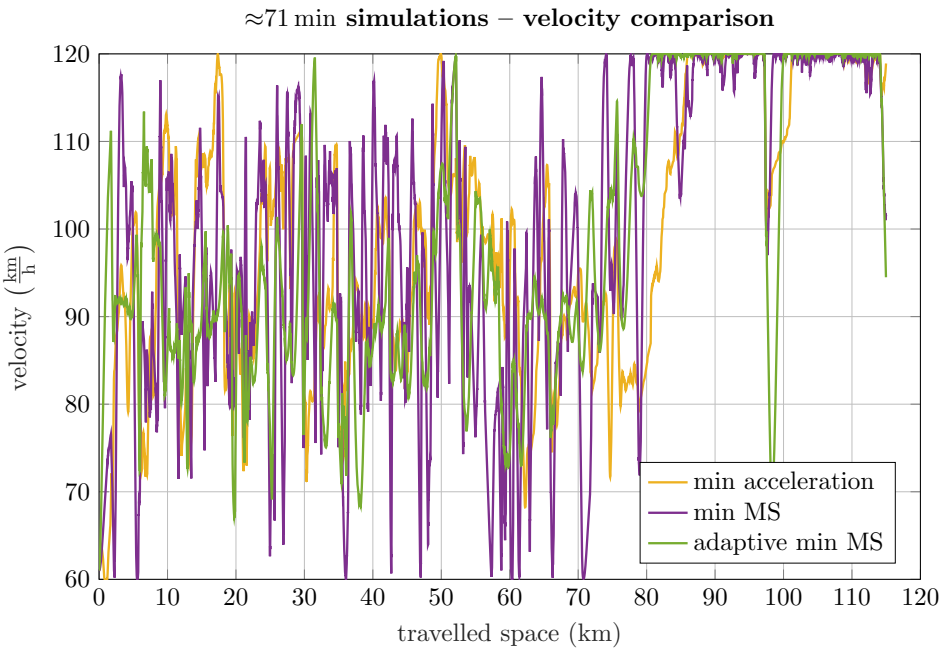

Figure 4.5: velocity of three cost functions with similar travel time

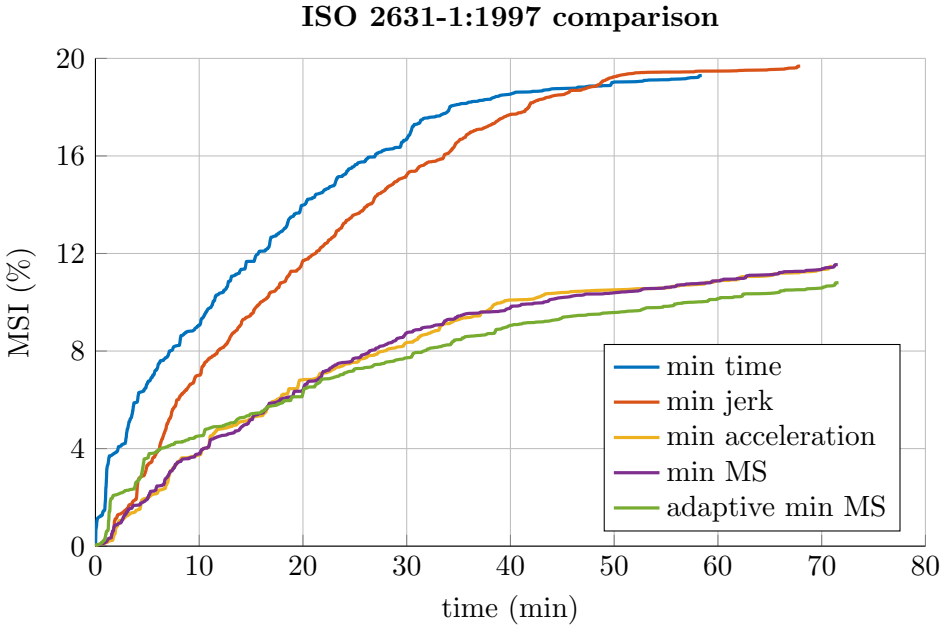

Figure 4.6: MSI estimated using the ISO-2631-1:1997 approach

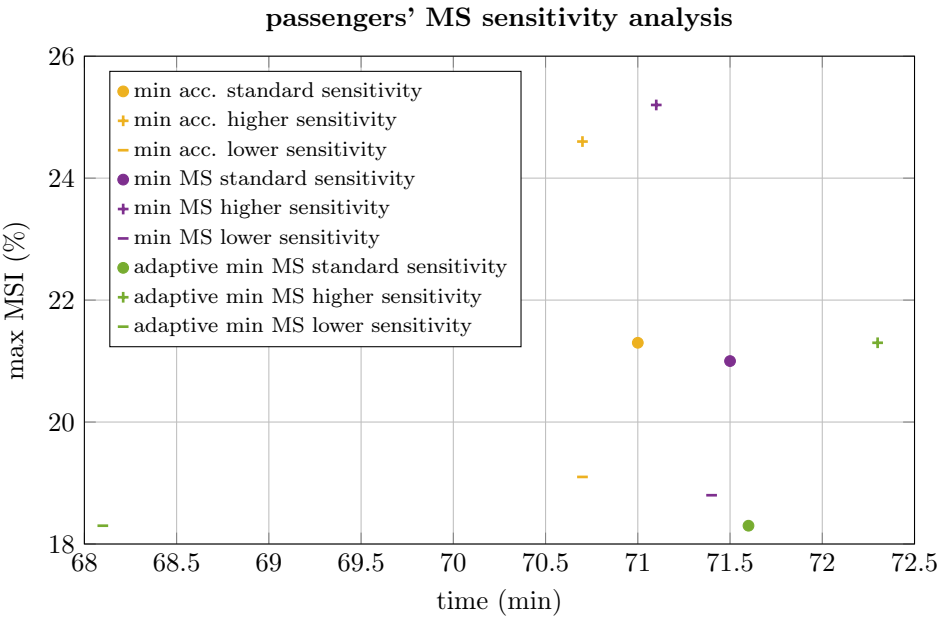

Figure 4.7: sensitivity analysis to different susceptibilities

Despite leading to similar results, is shown in [106] that the UniPG model fits much better the experimental results of [19, 107] compared to ISO 2631-1:1997; according to this, results in Fig. 4.1 are to be considered of general validity.

The usage of a Bos and Bles-derived model for the computation of the MSI to be used in the cost function is key to model the decrease in MSI in straight stretches that follow winding sections, which is important in the adaptive cost function. Using ISO-like modelling would have led to an indefinitely increasing MSI over time, resulting in an unjustified slowing down of the vehicle on any straight stretch that follows tortuous sections; while it is a common experience that without, or with small enough stimuli, the sickness will eventually decrease.

The results shown in Fig. 4.5 are used to understand how the different strategies adapt when varying the non-linear weighting, mimicking different susceptibilities. The non-linear weighting parameter b has been varied from 0.7 to 0.6 and 0.8 to model greater and lower susceptibility respectively. The results in Fig. 4.7 show that the minimum acceleration strategy and the base minimum MS one have similar performances. The adaptative MS strategy performs the best across all the susceptibility range studied; for low susceptibilities, the adaptive strategy is 3 min faster while having similar MSI (even slightly lower one), in the high susceptibility scenario, the adaptive cost function is 1.5 min slower but has 4% lower MSI than the other strategies. The consistency of the results when modelling different susceptibilities demonstrates that the difference between strategies' effectiveness is a general result.

The results of this research show that it is possible to improve passengers comfort and to reduce the MSI by taking into account comfort-related terms during mission planning. It is shown how modelling their physiological dynamics is not mandatory to reduce the MSI, but using a numerical model with the proposed adaptative cost

function is essential to have good performance and efficiency.

The novel methodology proposed for mission speed profile optimisation is the main contribution of this chapter, introducing MS-related terms in the vehicle performance definition.

The systematic comparison of the possible cost functions to reduce the MSI while minimising travel time is another contribution, demonstrating that it is possible to reduce the MSI without modelling its dynamics. The adaptive approach is, however, the most innovative one, explicitly introducing MS numerical models in the speed profile definition. This allows for fine-tuning with small variations of the motion-sickness-related cost and the best performance in terms of both incidence reduction and minimal travel time.

The last minor contribution is the definition of a space-integrated version of the UniPG model, which can be used in speed profile optimisation in hierarchical control systems like [156].

4.5 Conclusion

This chapter introduced a new approach to optimising the speed profile on a given path; reducing MSI while still minimising travel time can significantly improve the acceptance of automated driving technologies. The same approach can be used to improve the comfort for human-driven cars by recommending the best speed to the driver; or to improve services such as intercity buses or trains by implementing MS estimates during timetables planning. The proposed approach is not limited to autonomous vehicles, given the simple vehicle model.

The proposed techniques can be integrated into motion planning algorithms for AD control to extend their benefits when the path definition is computed in real-time and not a priori defined like in this chapter.

To give the possibility to the users to interactively fine-tune the trade-off between MS and travel time minimisation, like in an adaptive cost function, may greatly improve users' acceptance for autonomous vehicles. Thus might improve their adoption, with the resulting benefits in terms of safety and environmental impact of transportation.

Content related to this chapter has been presented in conferences and journal articles [155, 157].

Chapter 5

Trajectory optimisation for carsickness reduction

5.1 Introduction

In the previous chapter, it has been demonstrated how introducing MS related terms into vehicle control strategies can significantly contribute to preventing carsickness. In the previous chapter and in the literature [124] is shown how optimising the vehicle velocity reduces the MSI; which is an approach applicable to autonomous and human-driven cars. However, since autonomous cars are controlled by algorithms, they offer a wider range of possibilities.

In the literature [121, 123] MS-related terms are used in the vehicle control to reduce the MS; however, this combines the faster vehicle dynamics with the very slow dynamics typical of MS. The more complex control system proposed would eventually run at a slower rate, complicating the control of the vehicle dynamics.

In this chapter, is analysed how the issue of MS assessment may be dealt at higher levels, like the motion planning ones. During motion planning, the vehicle description is simplified to address different issues like road boundaries, obstacle avoidance, road rules compliance and, to a certain extent, vehicle performance. Is it possible to reduce MS during motion planning so that the lower control levels can take into account only the vehicle dynamics?

Varaiya [158] defines motion planning as a stack of different tasks to be performed to create a reference for the control algorithms; these tasks are:

1. route planning
2. path planning
3. manoeuvre choice
4. trajectory planning

The tasks are ordered from very high-level strategic tasks to lower-level planning ones, creating the reference for the control tasks; trajectory planning creates a reference for the control layers. While the control layers tracking deals with the vehicle dynamics and disturbances rejection, the reference guarantees that the path

is clear of obstacles and is *the best* path possible, where *the best* is chosen according to some kind of metrics.

In [159], a review of the main techniques used in trajectory planning is presented, dividing them into two main categories. In the first family the geometric curve used is restricted to a certain type and a piecewise path is constructed, optimising it by taking into account things like maximum acceleration and obstacles (e.g. [160, 161]); the second family uses a MPC approach to optimise the trajectory using techniques derived from control theory (e.g. [162–165]).

5.1.1 Research aim: MS reduction in motion planning

The research aim is to extend the MPC approaches to address the issue of MS in autonomous vehicles: can the problem of trajectory planning be exploited to address the issue of MS in autonomous cars? And if so, is it more effective and/or efficient to optimise the trajectory compared to a more general approach like the speed profile optimisation already analysed in the literature?

5.2 Methods

To understand how the trajectory can influence carsickness, a simulation approach has been used. The problem has been posed as a series of non-linear optimisation problems; by using the MATLAB MPC toolbox and the *fmincon* solver, the problem is formulated as a NMPC problem with a 6 s horizon. The simulations are run with a 2 Hz step size to accurately model the MS dynamics.

A perfect description of the simulated models is assumed. Therefore, each step takes as initial states the first predicted step of the previous optimisation. The only exception is the travelled space variable θ; after every optimisation, the point of the centerline nearest to the first predicted step is searched to set the right value for the next time step, avoiding integration drifting.

Different MS reduction strategies have been implemented in the same NMPC by using different cost functions in the optimisation. The results of several simulations using each of the cost functions are compared. Such comparison shows whether such optimisation may be effective in reducing the MSI.

Since the trajectory optimisation problem optimises the full trajectory (both the "racing line" and the vehicle velocity), an analysis is needed to understand how big is the contribution of the racing line compared to the one of the velocity profile. To perform this analysis, the accelerations of traversing the minimum-time racing line using the speed profile of the model-based MS reduction optimisation are computed, with the associated MSI. The difference in MSI between moving on the track according to the optimal trajectory, and moving on the minimum time racing line with the speed profile of the optimal trajectory, is used as a proxy to estimate the benefits of optimising the trajectory instead of optimising only the speed profile.

5.2.1 Road

The track used in the simulations, shown in Fig. 5.1, is a circuit represented by an x-y map, neglecting any vertical contribution; from the x-y map, a set of piecewise cubic polynomials is extracted to describe the x,y coordinates along the track, their

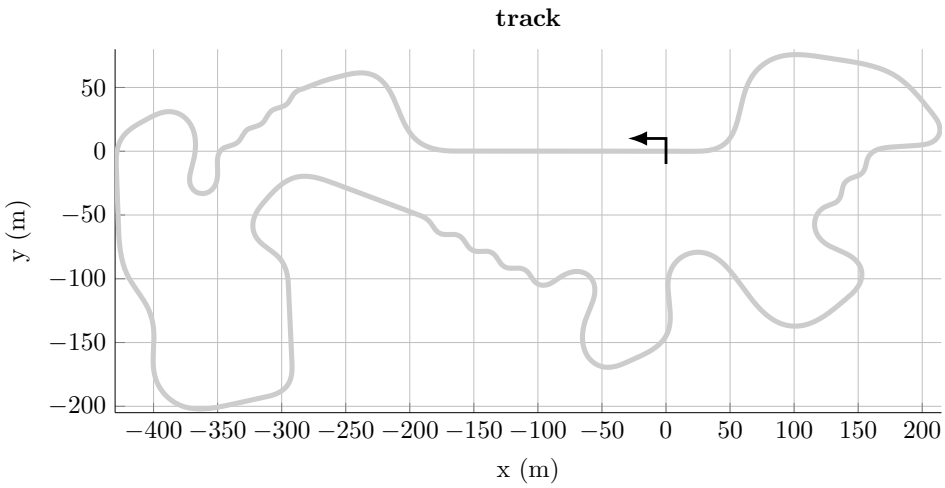

Figure 5.1: track overview

jacobian and hessian and the curvature. The simulation is six laps long for a total length of ≈13 km.

5.2.2 System dynamics

Vehicle model

Similarly to the previous chapter, the vehicle dynamics are represented by a point-mass model; however, in this chapter, the dynamics is time-defined. The point-mass dynamics are defined in a stationary reference frame and the vehicle accelerations (a_x, a_y) are the inputs of the MPC problem.

$$\begin{cases} \dot{x} = v_x \\ \dot{y} = v_y \\ \dot{v}_x = a_x \\ \dot{v}_y = a_y \end{cases} \tag{5.1}$$

Motion sickness model

As in the previous chapter, the MS model is the model presented in [106].

The non-linear Hill function and the MSI generation dynamics are the same as the previous chapter, respectively presented in Eq. (4.5) and in Eq. (4.6); therefore, for the sake of brevity, are not reported in this chapter.

The longitudinal and lateral conflicts dynamics are instead slightly different from the previous chapter ones, because the longitudinal and lateral accelerations (a_t, a_n) are derived from the accelerations in the absolute reference frame (a_x, a_y). The point mass dynamics are defined in a standing reference system, while the MS model takes as inputs the accelerations in the vehicle reference system. The latter are obtained rotating the system inputs shown Eq. (5.1), as shown in Eq. (5.2).

$$\begin{pmatrix} a_t \\ a_n \end{pmatrix} = \begin{pmatrix} \cos\left(\arctan2\left(v_y, v_x\right)\right) & \sin\left(\arctan2\left(v_y, v_x\right)\right) \\ -\sin\left(\arctan2\left(v_y, v_x\right)\right) & \cos\left(\arctan2\left(v_y, v_x\right)\right) \end{pmatrix} \begin{pmatrix} a_x \\ a_y \end{pmatrix} \tag{5.2}$$

Eq. (4.4) using the inputs defined in Eq. (5.2) becomes Eq. (5.3).

$$\begin{cases} \dot{c}_{t_1} = \alpha_1 c_{t_1} + \alpha_2 c_{t_2} + \alpha_3 c_{t_3} + a_t \\ \dot{c}_{t_2} = c_{t_1} \\ \dot{c}_{t_3} = c_{t_2} \\ \dot{c}_{n_1} = \alpha_1 c_{n_1} + \alpha_2 c_{n_2} + \alpha_3 c_{n_3} + a_n \\ \dot{c}_{n_2} = c_{n_1} \\ \dot{c}_{n_3} = c_{n_2} \end{cases} \tag{5.3}$$

where

$$\begin{cases} c_t = \gamma_1 c_{t_1} + \gamma_2 c_{t_2} \\ c_n = \gamma_1 c_{n_1} + \gamma_2 c_{n_2} \end{cases}$$

Travelled space

The reference path is parametrised by its arc length θ as in [163] to compute the vehicle distance from the centerline.

The travelled distance is updated projecting the vehicle velocity on the centerline as shown in Eq. (5.4), where $\left(v_x^\star, v_y^\star\right)$ are the jacobian respect to the arc length θ of the coordinates $(x^\star, y^\star)$ of the centerline

$$\begin{gathered} \dot{\theta} = \frac{\left(v_x, v_y\right) \cdot \left(v_x^\star, v_y^\star\right)}{\left\| v_x^\star, v_y^\star \right\|_2} \\ \text{where} \\ v_x^\star = \frac{\mathrm{d}x^\star}{\mathrm{d}\theta} \\ v_y^\star = \frac{\mathrm{d}y^\star}{\mathrm{d}\theta} \end{gathered} \tag{5.4}$$

However, this projection does not guarantee the exact identification of the centerline closest point to the vehicle, resulting in a small error. Therefore, after the optimisation routine, the travelled space variable is updated, searching in a neighbourhood of the predicted value the closest point to the new vehicle coordinates.

$$\theta_{k+1} = \arg\min_{\theta} \left(x_{k+1} - x^\star\left(\theta\right)\right)^2 + \left(y_{k+1} - y^\star\left(\theta\right)\right)^2 \tag{5.5}$$

5.2.3 Constraints

Similarly to the previous chapter, the vehicle is constrained to have an acceleration lower than 0.3 g.

The vehicle is also constrained to be within 2 m from the centerline.

$$\begin{cases} a_x^2 + a_y^2 - \left(0.3\,\mathrm{g}\right)^2 \leq 0 \\ \left(x - x^\star\left(\theta\right)\right)^2 + \left(y - y^\star\left(\theta\right)\right)^2 - \left(2\,\mathrm{m}\right)^2 \leq 0 \end{cases} \tag{5.6}$$

5.2.4 Cost functions

As in the previous chapter, the compared strategies are implemented in several cost functions. Given the results of the previous chapter, for the trajectory optimisation problem, only the best performing strategies of the previous chapter were chosen, namely:

1. minimum time cost function
2. minimum acceleration cost function
3. adaptive minimum instantaneous disturbance cost function

Minimum time strategy

Similarly to the previous chapter, the minimum time strategy is composed of a term minimising the travel time and a second one with a small cost on the manipulated variables. Given the fact that the trajectory is not constrained, like in the previous chapter, the minimum travel time and the maximum velocity targets are different. In [166] is analysed how only balancing between maximal travelled space and maximal exit velocity from the prediction horizon leads to a globally optimal minimum time strategy. The minimum time is done by maximising the travelled space variable θ at the end of the prediction horizon; neglecting, for the sake of simplicity, the trade-off analysed in [166].

$$J_k = C_t \left(\theta_k - \tilde{\theta}_{k+12|k} \right) + \sum_{n=1}^{12} C_u \left(\tilde{a}^2_{x_{k+n-1|k}} + \tilde{a}^2_{y_{k+n-1|k}} \right) \tag{5.7}$$

Minimum acceleration strategy

The acceleration strategy, as in the previous chapter was the minimum jerk one, is structurally identical to the minimum time function; however, the cost C_u on the input is replaced with a larger cost C_a aiming to reduce the accelerations to lower the MSI.

$$J_k = C_t \left(\theta_k - \tilde{\theta}_{k+12|k} \right) + \sum_{n=1}^{12} C_a \left(\tilde{a}^2_{x_{k+n-1|k}} + \tilde{a}^2_{y_{k+n-1|k}} \right) \tag{5.8}$$

Adaptive minimum MS strategy

This cost function adds to the minimum time one the MS-related cost using the MSI and the instantaneous disturbance introduced in the previous chapter.

$$J_k = C_t \left(\theta_k - \tilde{\theta}_{k+12|k} \right) + \sum_{n=1}^{12} C_u \left(\tilde{a}^2_{x_{k+n-1|k}} + \tilde{a}^2_{y_{k+n-1|k}} \right) + C_{MS} \widetilde{\mathrm{MSI}}_{k+n|k} \tilde{h}_{k+n|k} \tag{5.9}$$

Table 5.1: costs used in the reported simulations

$\mathbf{C_t}$	$\mathbf{C_u}$	$\mathbf{C_a}$	$\mathbf{C_{MS}}$
1	$1e^{-6}$	0.5	0.05

5.2.5 Composing the MPC problem

The MPC problem is built by assembling the parts explained in the previous paragraphs; the system dynamics are composed by the vehicle dynamics (including the travelled space estimation), the blocks of the conflict dynamics equations, a Hill function and the MSI dynamics equations. Composing the system dynamics to the constraints and cost functions described above leads to the formulation described in Eq. (5.10).

$$\begin{gathered} \min_{x,u} J_k \\ \\ \text{subject to:} \\ x_0 = x(0) \\ x_{k+1} = f\left(x_k, u_k\right) \\ a_x^2 + a_y^2 - \left(0.3\,\mathrm{g}\right)^2 \leq 0 \\ \left(x - x^\star\left(\theta\right)\right)^2 + \left(y - y^\star\left(\theta\right)\right)^2 - \left(2\,\mathrm{m}\right)^2 \leq 0 \end{gathered} \tag{5.10}$$

5.2.6 Performance assessment

To evaluate the cost functions performances the evolution of MSI over time is considered: the lower the travel time and the maximum MSI the better. Since the travelled distance is quite short when compared to MS characteristic timings, the MSI obtained during the simulation are extrapolated in two ways:

- by computing the MS evolution by propagating a null instantaneous disturbance to model how the MSI evolves when the motion stops after 13 km,
- by computing the average instantaneous disturbance over the last lap and computing the steady-state MSI with such continuous disturbance to model an indefinite long motion similar to the last lap. This method tends to overestimate the MSI of adaptive strategies like the model-based reduction one because, in such strategies, the disturbance decreases when the MSI increases; therefore, the disturbance decreases over time until the steady-state MSI is reached.

The costs of the simulations showed in the following section are reported in Table 5.1.

5.3 Results

The results, summarised in Fig. 5.2, show that the maximum MSI is reached some minutes after the motion stops; by extrapolating the MSI over several minutes, it can be seen that the lowest maximum MSI is reached by the model-based strategy, performing the best between the three cost functions. Interestingly, it has the

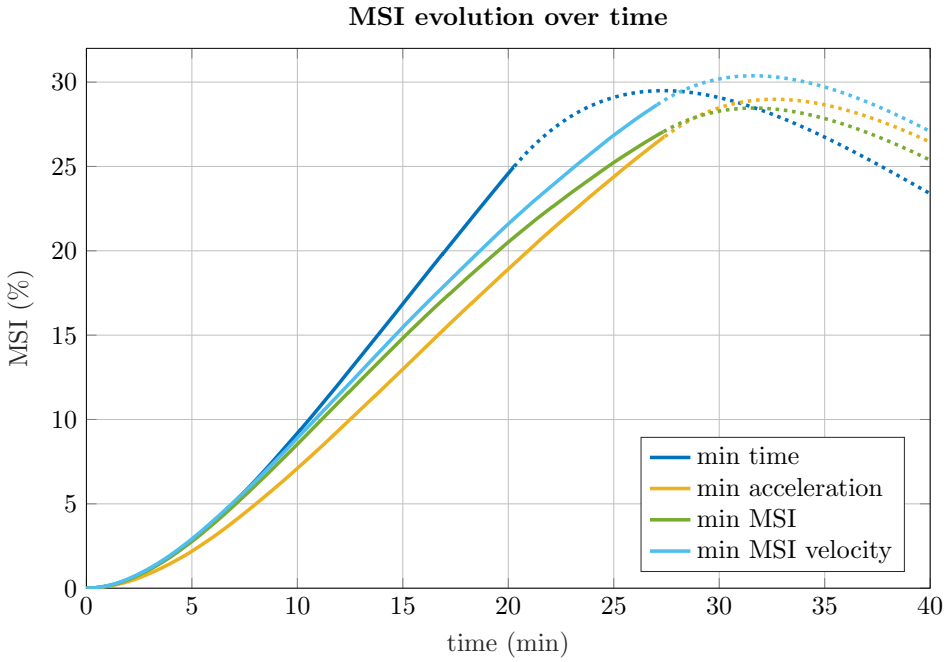

Figure 5.2: comparison of proposed cost function – MSI evolution over time

Table 5.2: cost functions performance

cost function	**MSI at stop**	**maximum MSI**	**steady-state MSI**
minimum time	25.0%	29.5%	63.6%
minimum acceleration	26.8%	29.0%	48.7%
minimum MSI	27.1%	28.5%	40.4%
min time traj + min MSI vel	28.7%	30.4%	51.2%

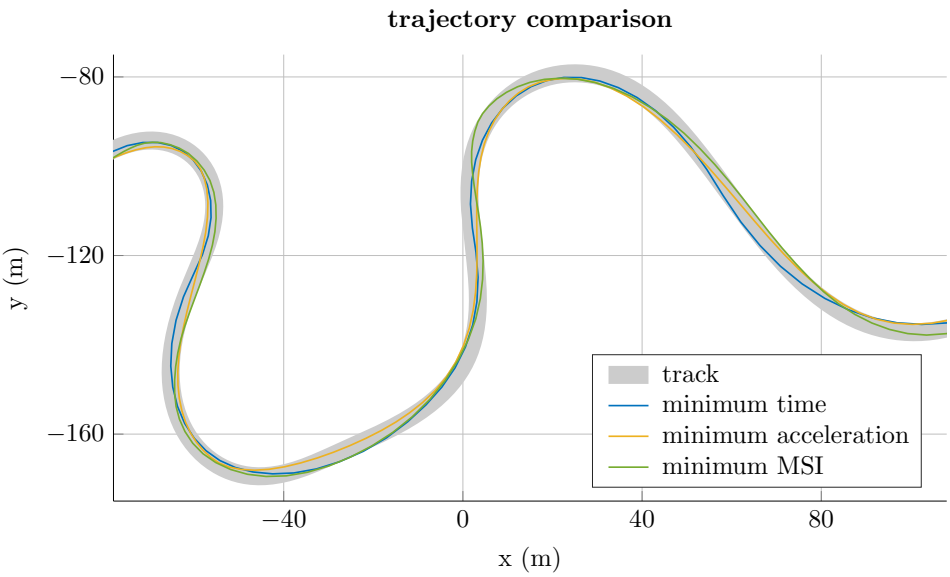

Figure 5.3: comparison of the different trajectories – turns 28 to 32

highest MSI at the very end of the motion, but since it has the lowest instantaneous disturbance during the last lap, the MSI has a smaller increase when the motion stops.

Paths longer than the one used in this chapter can benefit greatly by using these optimisation techniques: when extrapolating the results for an indefinite long path, by using the average instantaneous disturbance of the last lap and looking at the steady-state response, it can be seen that the MSI can range between $\approx 64\%$ of the minimum time cost function, the $\approx 49\%$ of the minimum acceleration cost function and the $\approx 40\%$ of the minimum acceleration cost function; when looking at the minimum MSI velocities applied over the minimum time trajectory, the steady-state MSI tends to $\approx 51\%$, showing that the trajectory optimisation, being it model-based or not, can reduce the MSI, furthermore, the reduction of MSI given by the trajectory optimisation does not increase the travel time when compared with a simple speed profile optimisation; improving the efficiency of the MSI reduction strategy in terms of travel time.

The results are summarized in Table 5.2.

In Fig. 5.3 is shown some turns of the last lap for each cost function; the trajectories of the several cost functions differ quite significantly, and in some cases like in turn 31, the trajectories approach the apex in very different ways.

In Fig. 5.4 the velocities of the last lap are shown; the minimum time cost function has the highest one, while the minimum acceleration strategy and the minimum MSI one have similar behaviour.

In Fig. 5.5 are shown the periodogram PSD estimates of the last lap accelerations for the different cost functions; the minimum time cost function has the highest PSD across all frequencies. It is interesting how, especially for the lateral acceleration a_n, the minimum MSI strategy has a lower PSD than the minimum acceleration strategy between 0.1 Hz to 0.2 Hz, which are the most provocative frequencies for MS, while are fairly similar outside this range. It should be noted that with a

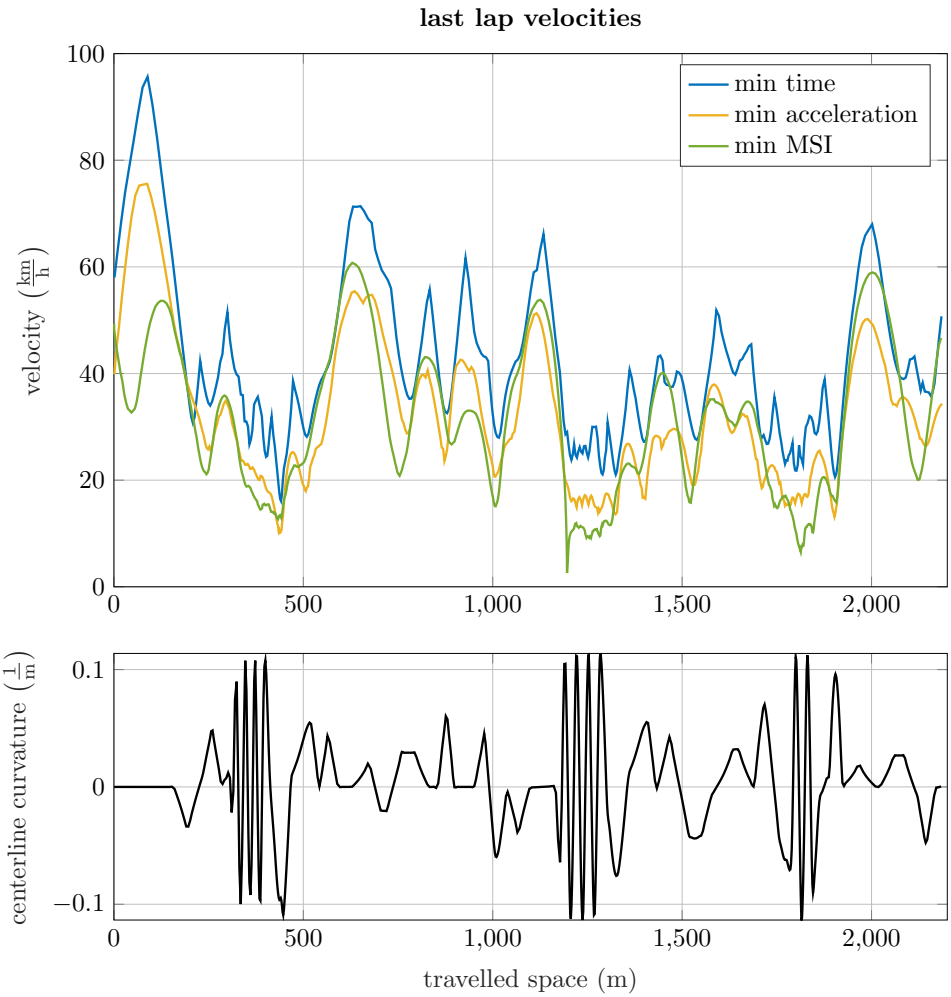

Figure 5.4: last lap velocity for the different cost functions

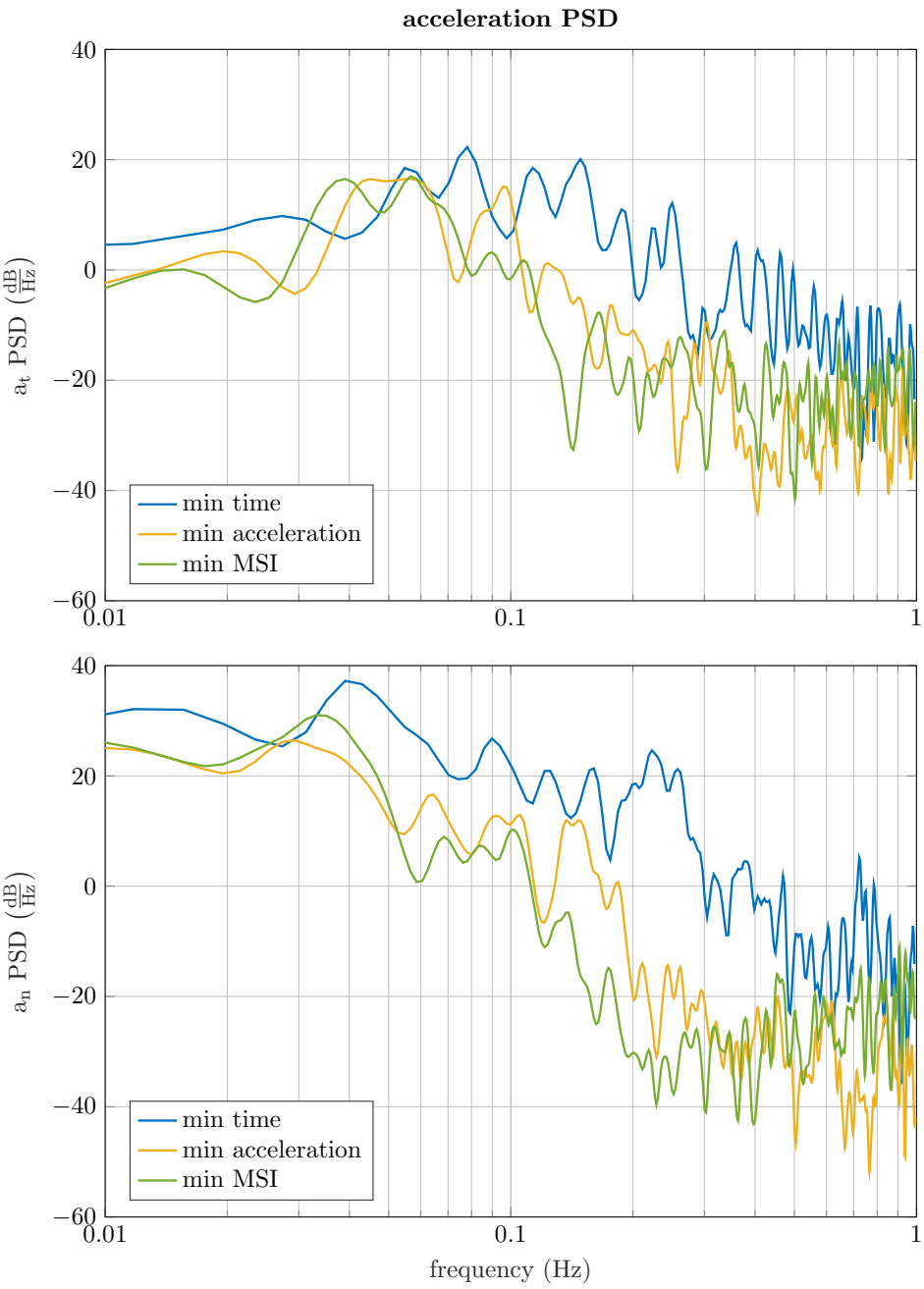

Figure 5.5: power spectral density estimation of the last lap accelerations for the different cost functions

prediction horizon of just 6 s it is impossible to optimise for lower frequency bands. The PSD of the longitudinal acceleration a_t of the minimum MSI strategy is slightly lower than the one of the minimum acceleration strategy in the 0.1 Hz to 0.2 Hz band, differently from the previous chapter results.

5.4 Discussion

The improvement over the minimum time approach shown in the results demonstrates that comfort-oriented motion planning can be beneficial to MS reduction in autonomous vehicles.

The results confirm that a model-based strategy is the most effective and efficient approach in reducing MS; the reduction of the acceleration is an effective strategy, but it leads to a greater increase in travel time compared to the model-based strategy.

The high performance of the model-based strategy suggests that the fairly short (when compared to the lower frequencies of the MS phenomenon) prediction horizon used in the NMPC does not compromise the effectiveness of the model-based approach. This means that this strategy is feasible in a real application, where the size of the optimisation problem is limited by the perception of the surrounding environment and by the control loop frequency.

Another important aspect of the results is that using the UniPG model without the visual-vestibular conflict is still effective in reducing the MS. So, it is possible to avoid the use of more complex models like the UniPG SeMo model (with the visual-vestibular interaction) presented in [106] or the one presented in [108] with both the angular velocities and linear accelerations.

The comparison between the model-based optimisation and using only its speed profile in the minimum time trajectory allows us to understand the effect of the trajectory in the MS reduction problem. Having much lower MSI than the speed profile while having nearly the same travel time shows that optimising the trajectory increase the efficiency of the MS reduction by allowing the same reduction in MSI but with lower travel time, or the same travel time but with a lower MSI.

The major contribution of this chapter is to introduce the issue of MS at the trajectory planning level while demonstrating its potential for MS reduction. Optimising the trajectory allows lower MSI while having almost any impact on travel time or computational complexity compared to just optimising the speed profile.

The increasing difference in MSI over time between the cost functions and the high difference in the steady-state response suggests that these MS reduction techniques are suited for travels longer than 20 min: due to the long time characteristic of the MS phenomenon, trying to optimise it in paths that have a travel time lower than 20 min does not give significant gains (if any) despite requiring the additional burden of computing the optimisation problem.

Another contribution is to generalise the behaviour of the proposed cost functions. In the previous chapter, several cost functions are compared to assess the best performers between the model-based ones and the ones not using an MS model. This chapter finds that the most efficient cost function in reducing the MSI is the one presented here as model-based, while the acceleration one is still effective despite being less efficient. This is coherent with the findings of the speed profile optimisation on a 120 km highway. In the previous chapter has also been shown the

consinstency of the cost functions performance when assessed with different MS models. Due to this coherency, it can be inferred that the goodness of such cost functions in optimising between time and MSI is general and not just related to the application shown in these chapters.

5.5 Conclusion

This chapter proves that taking into account passenger comfort during motion planning can be a significant step to reduce the discomfort in autonomous vehicles; using optimal methods to reduce MS can potentially increase the user acceptance of AD technology.

It is also shown how optimising the trajectory leads to better comfort than alternative reduction methods.

These benefits grow as the length of the route increases; therefore, such techniques are better suited for long travels. Using them in highway Advanced driver-Assistance Systems (ADAS) can be a suitable scenario where these optimisation techniques may be useful.

It is shown that using a model-based approach to the MS reduction problem is the most effective and efficient choice; however, in simpler implementation, just reducing the vehicle acceleration can be effective to limit the MS issue.

Chapter 6

Conclusion

In the present thesis the issue of MS has been analysed; to limit its impact in cars, several countermeasures from the literature have been discussed.

It is shown how the main countermeasures to MS are behavioural methods, like looking ahead and actively tilting the head, or the one related to the design of the vehicle and its interiors; these techniques are generally applicable to human-driven and autonomous cars, but they require a proactive approach from the passengers or are applicable only when designing new cars.

To overcome these issues, this thesis explores the main technologies to monitor MS in cars and how to control the vehicle to reduce the MSI.

Analysing the physiological signals related to MS, it emerges how to monitor carsickness two approaches are possible:

- monitoring the HRV to detect the sympathetic response related to MS
- estimating MSI using MS numerical models

In Section 3.1, the feasibility of camera-based HRV monitoring is analysed; using a photoplethysmograph, several techniques for HRV analysis are carried out, and the results are compared with a 60 Hz downsampling of the same data. The downsampling affects the peak identification; however, the HRV analysis has similar results, proving that a camera-based HRV analysis is possible.

In Section 3.2 the head inclination effect on MSI is discussed analysing how the results of Chapter 5 vary depending on the head inclination. It is shown how the head inclination has a significant effect; therefore, it is suggested how head pose estimation using cameras may correct the perceived accelerations fed to numerical models to take into account this effect.

To reduce MS in autonomous vehicles, in the last year, some work is starting questioning how to control the vehicle to combine low travel time with low MSI. In this thesis, Chapters 4 and 5 analyse how to optimise the vehicle motion to reduce the MSI while minimising travel times using theoretical based MS numerical models like the Bos and Bles-derived ones.

Chapter 4 covers the definition of the optimal speed profile on a given road to have the best trade-off between minimum travel time and minimum MSI. This method may address the issue of carsickness in autonomous cars being a reference for lower-level control layers or in human-driven ones can be used as a suggestion for the driver. The problem is formulated as a NMPC problem, and it has been

simulated on a 120 km motorway comparing different strategies. The results show that a model-based strategy taking into account the instantaneous disturbance and the MSI is the best way to prevent MS. Reducing vehicle accelerations is a simpler way to reduce the MSI; however, it is not as effective as the model-based strategy.

By narrowing the field to only autonomous vehicles, in Chapter 5 is analysed how addressing the issue of MS at the trajectory planning level may exploit the greater possibilities of autonomous cars to provide a less provocative experience to the passengers. The best performing strategies of Chapter 4 are translated for the trajectory optimisation problem and tested in a short and tortuous track; in this very different scenario, the results are coherent with the previous chapter ones, showing that the proposed strategies have general validity in reducing the MSI.

To summarising, the main contributions of this research activity are:

- proposing a novel methodology for the definition of an optimal speed profile for MS reduction; applicable in human-driven cars and autonomous ones,
- demonstrating the potential of MS-aware motion planning for autonomous vehicles, where the issue of MS is even more relevant,
- proposing and validating different strategies for MS reduction in different scenarios,
- introducing a space-integrated variant of the UniPG model
- determining the most feasible methods for MS monitoring in cars

The presented contributions are key to improve the knowledge and the techniques on reducing MS in cars. Since MS frequencies are typical of a car motion, it is utopian to completely prevent MS in cars; however, this study presents new ways to modify the car motion minimising its incidence on the passengers. These strategies are formulated in a way to be readily available for implementing them in ADAS or autonomous driving systems by introducing the MS-related strategies presented; this brings interesting perspectives in the development of human-focused driving automation systems.

The work presented in this thesis opens novel research topics to be developed in the following years, analysing the possible implementations of similar systems in real vehicles. Further analysis should be carried out analysing the effectiveness of the monitoring systems proposed and their robustness in the wild. Another open topic is the robustness of the camera-based cardiac pulse estimation to different light conditions and its racial robustness because the estimation is done analysing the skin colour.

The interaction between monitoring systems and reduction strategies is also an important research topic. Once the head acceleration monitoring techniques are implemented in vehicles, it is possible to modify the adaptive strategy proposed using the MSI derived from the head acceleration estimated using cameras. Furthermore, the balance between minimal time and minimal MSI can be modified when a shift in sympathetic activity related to MS is captured by analysing the passengers' HRV.

Bibliography

[1] N. A. Stanton and P. M. Salmon, 'Human error taxonomies applied to driving: A generic driver error taxonomy and its implications for intelligent transport systems', *Safety Science*, vol. 47, no. 2, pp. 227–237, Feb. 2009. DOI: 10/c4stzf.

[2] J. Carson, D. Adminaite-Fodor and G. Jost, 'Ranking EU progress on road safety: 14th road safety performance index report', 2020.

[3] T. Winkle, 'Safety Benefits of Automated Vehicles: Extended Findings from Accident Research for Development, Validation and Testing', in *Autonomous Driving*, M. Maurer, J. C. Gerdes, B. Lenz and H. Winner, Eds., Berlin, Heidelberg: Springer Berlin Heidelberg, 2016, pp. 335–364, ISBN: 978-3-662-48845-4. DOI: 10/dqsh.

[4] A. Simoes, 'Older Drivers and Driving Automation', in *Advances in Human Aspects of Transportation*, N. A. Stanton, Ed., vol. 597, Cham: Springer International Publishing, 2018, pp. 1082–1094, ISBN: 978-3-319-60440-4. DOI: 10.1007/978-3-319-60441-1_102.

[5] A. Talebpour and H. S. Mahmassani, 'Influence of connected and autonomous vehicles on traffic flow stability and throughput', *Transportation Research Part C: Emerging Technologies*, vol. 71, pp. 143–163, Oct. 2016. DOI: 10/f87kqp.

[6] R. E. Stern, Y. Chen, M. Churchill, F. Wu, M. L. Delle Monache, B. Piccoli, B. Seibold, J. Sprinkle and D. B. Work, 'Quantifying air quality benefits resulting from few autonomous vehicles stabilizing traffic', *Transportation Research Part D: Transport and Environment*, vol. 67, pp. 351–365, Feb. 2019. DOI: 10/ghg88q.

[7] D. J. Fagnant and K. M. Kockelman, 'The travel and environmental implications of shared autonomous vehicles, using agent-based model scenarios', *Transportation Research Part C: Emerging Technologies*, vol. 40, pp. 1–13, Mar. 2014. DOI: 10/f5wzwd.

[8] Z. Ning, F. Xia, N. Ullah, X. Kong and X. Hu, 'Vehicular Social Networks: Enabling Smart Mobility', *IEEE Communications Magazine*, vol. 55, no. 5, pp. 16–55, May 2017. DOI: 10/ghg883.

[9] J. Wan, D. Zhang, S. Zhao, L. Yang and J. Lloret, 'Context-aware vehicular cyber-physical systems with cloud support: Architecture, challenges, and solutions', *IEEE Communications Magazine*, vol. 52, no. 8, pp. 106–113, Aug. 2014. DOI: 10/ghg89m.

[10] F. Steck, V. Kolarova, F. Bahamonde-Birke, S. Trommer and B. Lenz, 'How Autonomous Driving May Affect the Value of Travel Time Savings for Commuting', *Transportation Research Record: Journal of the Transportation Research Board*, vol. 2672, no. 46, pp. 11–20, Dec. 2018. DOI: 10/gddr9h.

[11] P. Bansal, K. M. Kockelman and A. Singh, 'Assessing public opinions of and interest in new vehicle technologies: An Austin perspective', *Transportation Research Part C: Emerging Technologies*, vol. 67, pp. 1–14, Jun. 2016. DOI: 10/f8rh2j.

[12] W. Payre, J. Cestac and P. Delhomme, 'Intention to use a fully automated car: Attitudes and a priori acceptability', *Transportation Research Part F: Traffic Psychology and Behaviour*, vol. 27, pp. 252–263, Nov. 2014. DOI: 10/gfkv98.

[13] J. Hudson, M. Orviska and J. Hunady, 'People's attitudes to autonomous vehicles', *Transportation Research Part A: Policy and Practice*, vol. 121, pp. 164–176, Mar. 2019. DOI: 10/ghd58z.

[14] M. Sivak and B. Schoettle, 'Motion sickness in self-driving vehicles', The University of Michigan - Transportation Research Institute, UMTRI-2015-12, Apr. 2015.

[15] C. Diels and J. E. Bos, 'Self-driving carsickness', *Applied Ergonomics*, vol. 53, pp. 374–382, Mar. 2016. DOI: 10/gf4sn5.

[16] J. Iskander, M. Attia, K. Saleh, D. Nahavandi, A. Abobakr, S. Mohamed, H. Asadi, A. Khosravi, C. P. Lim and M. Hossny, 'From car sickness to autonomous car sickness: A review', *Transportation Research Part F: Traffic Psychology and Behaviour*, vol. 62, pp. 716–726, Apr. 2019. DOI: 10/ghf99r.

[17] C. Diels, J. E. Bos, K. Hottelart and P. Reilhac, 'Motion Sickness in Automated Vehicles: The Elephant in the Room', in *Road Vehicle Automation 3*, G. Meyer and S. Beiker, Eds., Cham: Springer International Publishing, 2016, pp. 121–129, ISBN: 978-3-319-40502-5. DOI: 10/dqsg.

[18] P. A. Singleton, 'Discussing the "positive utilities" of autonomous vehicles: Will travellers really use their time productively?', *Transport Reviews*, vol. 39, no. 1, pp. 50–65, 2nd Jan. 2019. DOI: 10/ggp9z2.

[19] J. F. O'Hanlon and M. E. McCauley, 'Motion Sickness Incidence as a Function of the Frequency and Acceleration of Vertical Sinusoidal Motion', Office of Naval Research, AD0768215, Sep. 1973.

[20] J. Golding, 'Motion sickness', in *Handbook of Clinical Neurology*, vol. 137, Elsevier, 2016, pp. 371–390, ISBN: 978-0-444-63437-5. DOI: 10.1016/B978-0-444-63437-5.00027-3.

[21] J. Irwin, 'The pathology of sea-sickness', *The Lancet*, vol. 118, no. 3039, pp. 907–909, Nov. 1881. DOI: 10/fnb6xz.

[22] A. Lawther and M. J. Griffin, 'The motion of a ship at sea and the consequent motion sickness amongst passengers', *Ergonomics*, vol. 29, no. 4, pp. 535–552, Apr. 1986. DOI: 10/fk9tsh.

[23] A. Wertheim, J. Bos and W. Bles, 'Contributions of roll and pitch to sea sickness', *Brain Research Bulletin*, vol. 47, no. 5, pp. 517–524, Nov. 1998. DOI: 10/czz9gg.

[24] M. Turner and M. J. Griffin, 'Motion sickness in public road transport: The relative importance of motion, vision and individual differences', *British Journal of Psychology*, vol. 90, no. 4, pp. 519–530, Nov. 1999. DOI: 10/bzgp56.

[25] M. Turner and M. J. Griffin, 'Motion sickness in public road transport: Passenger behavior and susceptibility', *Ergonomics*, vol. 42, no. 3, pp. 444–461, Mar. 1999. DOI: 10/fkz8vm. pmid: 10048305.

[26] M. Turner and M. J. Griffin, 'Motion sickness in public road transport: The effect of driver, route and vehicle', *Ergonomics*, vol. 42, no. 12, pp. 1646–1664, Dec. 1999. DOI: 10/c9rnw5. pmid: 10643406.

[27] P. Perrin, A. Lion, G. Bosser, G. Gauchard and C. Meistelman, 'Motion Sickness in Rally Car Co-Drivers', *Aviation, Space, and Environmental Medicine*, vol. 84, no. 5, pp. 473–477, 1st May 2013. DOI: 10/ggp867.

[28] J. Förstberg, E. Andersson and T. Ledin, 'Influence of different conditions for tilt compensation on symptoms of motion sickness in tilting trains', *Brain Research Bulletin*, vol. 47, no. 5, pp. 525–535, Nov. 1998. DOI: 10/c9jwz3.

[29] C. Braccesi, F. Cianetti and A. Elia, 'Motion sickness. Part II: Experimental verification on the railways of a model for predicting motion sickness incidence', *International Journal of Human Factors Modelling and Simulation*, vol. 2, no. 3, p. 188, 2011. DOI: 10/fxtpx6.

[30] C. Braccesi, F. Cianetti and R. Scaletta, 'Development of a Methodology for the Evaluation of Motion Sickness Incidence in Railways', ASME, 15th Nov. 2013, V013T14A045, ISBN: 978-0-7918-5642-0. DOI: 10/ggqc6s.

[31] B. Cohen, M. Dai, D. Ogorodnikov, J. Laurens, T. Raphan, P. Müller, A. Athanasios, J. Edmaier, T. Grossenbacher, K. Stadtmüller, U. Brugger, G. Hauser and D. Straumann, 'Motion sickness on tilting trains', *The FASEB Journal*, vol. 25, no. 11, pp. 3765–3774, Nov. 2011. DOI: 10/d38dcm.

[32] M. Turner, M. J. Griffin and I. Holland, 'Airsickness and aircraft motion during short-haul flights', *Aviation, Space, and Environmental Medicine*, vol. 71, no. 12, pp. 1181–1189, Dec. 2000. pmid: 11439716.

[33] A. Van Ombergen, B. D. Lawson and F. L. Wuyts, 'Motion sickness and sopite syndrome associated with parabolic flights: A case report', *International Journal of Audiology*, vol. 55, no. 3, pp. 189–194, 3rd Mar. 2016. DOI: 10/ghdcdm.

[34] C. M. Oman, 'Spacelab experiments on space motion sickness', *Acta Astronautica*, vol. 15, no. 1, pp. 55–66, Jan. 1987. DOI: 10/chs3mb.

[35] T. Russomano, M. da Rosa and M. A. Dos Santos, 'Space motion sickness: A common neurovestibular dysfunction in microgravity', *Neurology India*, vol. 67, S214–S218, Supplement May 2019. DOI: 10/ghdcd5. pmid: 31134912.

[36] L. R. Young, 'Visually induced motion in flight simulation', presented at the AGARD Symposioum on Flight Simulation, Brussels, 1978.

[37] J. K. Huang and L. R. Young, 'Influence of visual and motion cues on manual lateral stabilization', *Aviation, Space, and Environmental Medicine*, vol. 58, no. 12, pp. 1197–1204, Dec. 1987. pmid: 3426495.

[38] J. E. Bos, S. N. MacKinnon and A. Patterson, 'Motion sickness symptoms in a ship motion simulator: Effects of inside, outside, and no view', *Aviation Space and Environmental Medicine*, vol. 76, no. 12, pp. 1111–1118, 2005.

[39] J. F. Golding, S. Arun, E. Wortley, K. Wotton-Hamrioui, S. Cousins and M. A. Gresty, 'Off-Vertical Axis Rotation of the Visual Field and Nauseogenicity', *Aviation, Space, and Environmental Medicine*, vol. 80, no. 6, pp. 516–521, 1st Jun. 2009. DOI: 10/dfk7fh.

[40] B. Keshavarz, L. J. Hettinger, R. S. Kennedy and J. L. Campos, 'Demonstrating the Potential for Dynamic Auditory Stimulation to Contribute to Motion Sickness', *PLoS ONE*, vol. 9, no. 7, M. S. Malmierca, Ed., e101016, 1st Jul. 2014. DOI: 10/f6ghmg.

[41] O. X. Kuiper, J. E. Bos, C. Diels and E. A. Schmidt, 'Knowing what's coming: Anticipatory audio cues can mitigate motion sickness', *Applied Ergonomics*, vol. 85, p. 103 068, May 2020. DOI: 10/ggp88p.

[42] K. Zużewicz, A. Saulewicz, M. Konarska and Z. Kaczorowski, 'Heart rate variability and motion sickness during forklift simulator driving', *International journal of occupational safety and ergonomics: JOSE*, vol. 17, no. 4, pp. 403–410, 2011. DOI: 10/ggqc6t.

[43] O. X. Kuiper, J. E. Bos, C. Diels and K. Cammaerts, 'Moving base driving simulators' potential for carsickness research', *Applied Ergonomics*, vol. 81, p. 102 889, Nov. 2019. DOI: 10/ggp9bs.

[44] R. Lewkowicz, 'A centrifuge-based flight simulator: Optimization of a baseline acceleration profile based on the motion sickness incidence', *Acta Astronautica*, vol. 164, pp. 23–33, Nov. 2019. DOI: 10/ggp9bw.

[45] L.-L. Zhang, J.-Q. Wang, R.-R. Qi, L.-L. Pan, M. Li and Y.-L. Cai, 'Motion Sickness: Current Knowledge and Recent Advance', *CNS Neuroscience & Therapeutics*, vol. 22, no. 1, pp. 15–24, Jan. 2016. DOI: 10/f76z9v.

[46] S. Hu, K. A. McChesney, K. A. Player, A. M. Bahl, J. B. Buchanan and J. E. Scozzafava, 'Systematic investigation of physiological correlates of motion sickness induced by viewing an optokinetic rotating drum', *Aviation, Space, and Environmental Medicine*, vol. 70, no. 8, pp. 759–765, Aug. 1999. pmid: 10447048.

[47] I. M. Lang, S. K. Sarna and R. Shaker, 'Gastrointestinal motor and myoelectric correlates of motion sickness', *American Journal of Physiology-Gastrointestinal and Liver Physiology*, vol. 277, no. 3, G642–G652, 1st Sep. 1999. DOI: 10/ghfvzr.

[48] M. E. Levine, R. M. Stern and K. L. Koch, 'Enhanced perceptions of control and predictability reduce motion-induced nausea and gastric dysrhythmia', *Experimental Brain Research*, vol. 232, no. 8, pp. 2675–2684, Aug. 2014. DOI: 10/f6bv2k.

[49] P. J. Gianaros, K. S. Quigley, E. R. Muth, M. E. Levine, R. C. Vasko and R. M. Stern, 'Relationship between temporal changes in cardiac parasympathetic activity and motion sickness severity', *Psychophysiology*, vol. 40, no. 1, pp. 39–44, Jan. 2003. pmid: 12751802.

[50] S. Ohyama, S. Nishiike, H. Watanabe, K. Matsuoka, H. Akizuki, N. Takeda and T. Harada, 'Autonomic responses during motion sickness induced by virtual reality', *Auris Nasus Larynx*, vol. 34, no. 3, pp. 303–306, Sep. 2007. DOI: 10/bbgrjr.

[51] L. Lacount, V. Napadow, B. Kuo, K. Park, J. Kim, E. Brown and R. Barbieri, 'Dynamic Cardiovagal Response to Motion Sickness: A Point-Process Heart Rate Variability Study', *Computers in Cardiology*, vol. 36, pp. 49–52, 1st Jan. 2009. pmid: 20445767.

[52] C.-T. Lin, C.-L. Lin, T.-W. Chiu, J.-R. Duann and T.-P. Jung, 'Effect of respiratory modulation on relationship between heart rate variability and motion sickness', *Annual International Conference of the IEEE Engineering in Medicine and Biology Society. IEEE Engineering in Medicine and Biology Society. Annual International Conference*, vol. 2011, pp. 1921–1924, 2011. DOI: 10/dmfwxg. pmid: 22254707.

[53] C.-L. Lin, T.-P. Jung, S.-W. Chuang, J.-R. Duann, C.-T. Lin and T.-W. Chiu, 'Self-adjustments may account for the contradictory correlations between HRV and motion-sickness severity', *International Journal of Psychophysiology*, vol. 87, no. 1, pp. 70–80, Jan. 2013. DOI: 10/f4p4rq.

[54] L. A. Warwick-Evans, R. E. Church, C. Hancock, D. Jochim, P. H. Morris and F. Ward, 'Electrodermal activity as an index of motion sickness.', *Aviation, Space, and Environmental Medicine*, vol. 58, no. 5, pp. 417–423, 1987.

[55] H. Wan, S. Hu and J. Wang, 'Correlation of phasic and tonic skin-conductance responses with severity of motion sickness induced by viewing an optokinetic rotating drum', *Perceptual and Motor Skills*, vol. 97, pp. 1051–1057, 3 Pt 2 Dec. 2003. DOI: 10/fns2kf. pmid: 15002846.

[56] G. Nobel, A. Tribukait, I. B. Mekjavic and O. Eiken, 'Effects of motion sickness on thermoregulatory responses in a thermoneutral air environment', *European Journal of Applied Physiology*, vol. 112, no. 5, pp. 1717–1723, May 2012. DOI: 10/d52pmt.

[57] E. Nalivaiko, J. A. Rudd and R. H. So, 'Motion sickness, nausea and thermoregulation: The "toxic" hypothesis', *Temperature*, vol. 1, no. 3, pp. 164–171, 31st Dec. 2014. DOI: 10/ghfv5s.

[58] M. Varlet, B. G. Bardy, F.-C. Chen, C. Alcantara and T. A. Stoffregen, 'Coupling of postural activity with motion of a ship at sea', *Experimental Brain Research*, vol. 233, no. 5, pp. 1607–1616, May 2015. DOI: 10/f65fhr.

[59] H. J. Walter, R. Li, J. Munafo, C. Curry, N. Peterson and T. A. Stoffregen, 'Unstable coupling of body sway with imposed motion precedes visually induced motion sickness', *Human Movement Science*, Mar. 2019. DOI: 10/ghdcfs.

[60] M. Dennison and M. D'Zmura, 'Effects of unexpected visual motion on postural sway and motion sickness', *Applied Ergonomics*, vol. 71, pp. 9–16, Sep. 2018. DOI: 10/ghdcc5.

[61] C. D. Wood, 'Antimotion Sickness and Antiemetic Drugs:' *Drugs*, vol. 17, no. 6, pp. 471–479, Jun. 1979. DOI: 10/dh47gb.

[62] H. Suzuki, H. Shiroto and K. Tezuka, 'Effects of Low Frequency Vibration on Train Motion Sickness', *Quarterly Report of RTRI*, vol. 46, no. 1, pp. 35–39, 2005. DOI: 10/cswscb.

[63] A. Paillard, M. Lamôré, O. Etard, J.-L. Millot, L. Jacquot, P. Denise and G. Quarck, 'Is there a relationship between odors and motion sickness?', *Neuroscience Letters*, vol. 566, pp. 326–330, Apr. 2014. DOI: 10/f53cdv.

[64] A. Graybiel and J. Knepton, 'Sopite syndrome: A sometimes sole manifestation of motion sickness', *Aviation, Space, and Environmental Medicine*, vol. 47, no. 8, pp. 873–882, Aug. 1976. pmid: 949309.

[65] B. Lawson and A. Mead, 'The sopite syndrome revisited: Drowsiness and mood changes during real or apparent motion', *Acta Astronautica*, vol. 43, no. 3-6, pp. 181–192, Aug. 1998. DOI: 10/fsrtgm.

[66] J. F. Golding, 'Motion sickness susceptibility questionnaire revised and its relationship to other forms of sickness', *Brain Research Bulletin*, vol. 47, no. 5, pp. 507–516, Nov. 1998. DOI: 10/c985gh.

[67] A. Lawther and M. J. Griffin, 'A survey of the occurrence of motion sickness amongst passengers at sea', *Aviation, Space, and Environmental Medicine*, vol. 59, no. 5, pp. 399–406, May 1988. pmid: 3390095.

[68] S. Klosterhalfen, S. Kellermann, F. Pan, U. Stockhorst, G. Hall and P. Enck, 'Effects of ethnicity and gender on motion sickness susceptibility', *Aviation, Space, and Environmental Medicine*, vol. 76, no. 11, pp. 1051–1057, Nov. 2005. pmid: 16313141.

[69] J. T. Reason and J. J. Brand, *Motion Sickness*. London, New York: Academic Press, 1975, 310 pp., ISBN: 978-0-12-584050-7.

[70] I. F. Henriques, D. W. Douglas de Oliveira, F. Oliveira-Ferreira and P. M. O. Andrade, 'Motion sickness prevalence in school children', *European Journal of Pediatrics*, vol. 173, no. 11, pp. 1473–1482, Nov. 2014. DOI: 10/ghfwgn.

[71] R. S. Kennedy, J. E. Fowlkes, K. S. Berbaum and M. G. Lilienthal, 'Use of a motion sickness history questionnaire for prediction of simulator sickness', *Aviation, Space, and Environmental Medicine*, vol. 63, no. 7, pp. 588–593, Jul. 1992. pmid: 1616434.

[72] R. S. Kennedy, G. C. Tolhurst and A. Graybiel, 'The effects of visual deprivation on adaptation to a rotating environment. NSAM-918', *Research Report. Naval School of Aviation Medicine (U.S.)*, pp. 1–36, 18th Mar. 1965. pmid: 5294754.

[73] R. S. Kennedy, N. E. Lane, K. S. Berbaum and M. G. Lilienthal, 'Simulator Sickness Questionnaire: An Enhanced Method for Quantifying Simulator Sickness', *The International Journal of Aviation Psychology*, vol. 3, no. 3, pp. 203–220, Jul. 1993. DOI: 10/bbh54v.

[74] H. K. Kim, J. Park, Y. Choi and M. Choe, 'Virtual reality sickness questionnaire (VRSQ): Motion sickness measurement index in a virtual reality environment', *Applied Ergonomics*, vol. 69, pp. 66–73, May 2018. DOI: 10/gc96dc.

[75] M. Treisman, 'Motion sickness: An evolutionary hypothesis', *Science (New York, N.Y.)*, vol. 197, no. 4302, pp. 493–495, 29th Jul. 1977. DOI: 10/bzz8cz. pmid: 301659.

[76] J. F. Golding, 'Motion sickness susceptibility', *Autonomic Neuroscience*, vol. 129, no. 1-2, pp. 67–76, Oct. 2006. DOI: 10/ft5h29.

[77] W. Bles, J. E. Bos, B. de Graaf, E. Groen and A. H. Wertheim, 'Motion sickness: Only one provocative conflict?', *Brain Research Bulletin*, vol. 47, no. 5, pp. 481–487, Nov. 1998. DOI: 10/bzzgrr.

[78] G. E. Riccio and T. A. Stoffregen, 'An ecological Theory of Motion Sickness and Postural Instability', *Ecological Psychology*, vol. 3, no. 3, pp. 195–240, Sep. 1991. DOI: 10/c6scw3.

[79] T. A. Stoffregen and G. E. Riccio, 'An Ecological Critique of the Sensory Conflict Theory of Motion Sickness', *Ecological Psychology*, vol. 3, no. 3, pp. 159–194, Sep. 1991. DOI: 10/fnwwvr.

[80] C. M. Oman, 'Are evolutionary hypotheses for motion sickness "just-so" stories?', *Journal of Vestibular Research*, vol. 22, no. 2,3, pp. 117–127, 2012. DOI: 10/ghft3b.

[81] P. S. Cowings and W. B. Toscano, 'Autogenic-feedback training exercise is superior to promethazine for control of motion sickness symptoms', *Journal of Clinical Pharmacology*, vol. 40, no. 10, pp. 1154–1165, Oct. 2000. pmid: 11028255.

[82] M. Lucertini, P. Verde and P. Trivelloni, 'Rehabilitation from Airsickness in Military Pilots: Long-Term Treatment Effectiveness', *Aviation, Space, and Environmental Medicine*, vol. 84, no. 11, pp. 1196–1200, 1st Nov. 2013. DOI: 10/f5ms7w.

[83] F. Y. P. Sang, J. Billar, M. A. Gresty and J. F. Golding, 'Effect of a Novel Motion Desensitization Training Regime and Controlled Breathing on Habituation to Motion Sickness', *Perceptual and Motor Skills*, vol. 101, no. 1, pp. 244–256, Aug. 2005. DOI: 10/b45ktj.

[84] L. Murdin, J. Golding and A. Bronstein, 'Managing motion sickness', *BMJ*, vol. 343, pp. d7430–d7430, dec02 1 2nd Dec. 2011. DOI: 10/dpqfsx.

[85] M. Dai, T. Raphan and B. Cohen, 'Prolonged reduction of motion sickness sensitivity by visual-vestibular interaction', *Experimental Brain Research*, vol. 210, no. 3-4, pp. 503–513, May 2011. DOI: 10/bjnfs9.

[86] E. Ressiot, M. Dolz, L. Bonne and R. Marianowski, 'Prospective study on the efficacy of optokinetic training in the treatment of seasickness', *European Annals of Otorhinolaryngology, Head and Neck Diseases*, vol. 130, no. 5, pp. 263–268, Nov. 2013. DOI: 10/f5v8p2.

[87] C. V. Rizzo-Sierra, A. Gonzalez-Castaño and F. E. Leon-Sarmiento, 'Galvanic vestibular stimulation: A novel modulatory countermeasure for vestibular-associated movement disorders', *Arquivos de Neuro-Psiquiatria*, vol. 72, no. 1, pp. 72–77, Jan. 2014. DOI: 10/f529g9.

[88] V. Dilda, H. G. MacDougall and S. T. Moore, 'Tolerance to Extended Galvanic Vestibular Stimulation: Optimal Exposure for Astronaut Training', *Aviation, Space, and Environmental Medicine*, vol. 82, no. 8, pp. 770–774, 1st Aug. 2011. DOI: 10/b9qn23.

[89] M. J. Cevette, J. Stepanek, D. Cocco, A. M. Galea, G. N. Pradhan, L. S. Wagner, S. R. Oakley, B. E. Smith, D. A. Zapala and K. H. Brookler, 'Oculo-Vestibular Recoupling Using Galvanic Vestibular Stimulation to Mitigate Simulator Sickness', *Aviation, Space, and Environmental Medicine*, vol. 83, no. 6, pp. 549–555, 1st Jun. 2012. DOI: 10/f3z8tf.

[90] F. D. Yen Pik Sang, J. P. Billar, J. F. Golding and M. A. Gresty, 'Behavioral methods of alleviating motion sickness: Effectiveness of controlled breathing and a music audiotape', *Journal of Travel Medicine*, vol. 10, no. 2, pp. 108–111, Mar. 2003. DOI: 10.2310/7060.2003.31768. pmid: 12650654.

[91] F. D. Yen Pik Sang, J. F. Golding and M. A. Gresty, 'Suppression of sickness by controlled breathing during mildly nauseogenic motion', *Aviation, Space, and Environmental Medicine*, vol. 74, no. 9, pp. 998–1002, Sep. 2003. pmid: 14503682.

[92] T. Wada, S. Fujisawa, K. Imaizumi, N. Kamiji and S. Doi, 'Effect of Driver's Head Tilt Strategy on Motion Sickness Incidence', *IFAC Proceedings Volumes*, vol. 43, no. 13, pp. 192–197, 2010. DOI: 10/dkfpqf.

[93] T. Wada, H. Konno, S. Fujisawa and S. Doi, 'Can Passengers' Active Head Tilt Decrease the Severity of Carsickness?: Effect of Head Tilt on Severity of Motion Sickness in a Lateral Acceleration Environment', *Human Factors: The Journal of the Human Factors and Ergonomics Society*, vol. 54, no. 2, pp. 226–234, Apr. 2012. DOI: 10/ghdccq.

[94] T. Wada and K. Yoshida, 'Effect of passengers' active head tilt and opening/closure of eyes on motion sickness in lateral acceleration environment of cars', *Ergonomics*, vol. 59, no. 8, pp. 1050–1059, 2nd Aug. 2016. DOI: 10/ghdcc4.

[95] J. F. Golding, H. M. Markey and J. R. Stott, 'The effects of motion direction, body axis, and posture on motion sickness induced by low frequency linear oscillation', *Aviation, Space, and Environmental Medicine*, vol. 66, no. 11, pp. 1046–1051, Nov. 1995. pmid: 8588793.

[96] C.-H. Chang, W.-W. Pan, F.-C. Chen and T. A. Stoffregen, 'Console video games, postural activity, and motion sickness during passive restraint', *Experimental Brain Research*, vol. 229, no. 2, pp. 235–242, Aug. 2013. DOI: 10/f45thb.

[97] A. Rolnick and R. E. Lubow, 'Why is the driver rarely motion sick? The role of controllability in motion sickness', *Ergonomics*, vol. 34, no. 7, pp. 867–879, Jul. 1991. DOI: 10/c78bgz.

[98] C. M. Oman, 'A heuristic mathematical model for the dynamics of sensory conflict and motion sickness', *Acta Oto-Laryngologica. Supplementum*, vol. 392, pp. 1–44, 1982. pmid: 6303041.

[99] J. E. Bos and W. Bles, 'Theoretical considerations on canal-otolith interaction and an observer model', *Biological Cybernetics*, vol. 86, no. 3, pp. 191–207, 1st Mar. 2002. DOI: 10/cf7tcq.

[100] C. M. Webb, A. Estrada and J. R. Athy, 'Motion Sickness Prevention by an 8-Hz Stroboscopic Environment During Air Transport', *Aviation, Space, and Environmental Medicine*, vol. 84, no. 3, pp. 177–183, 1st Mar. 2013. DOI: 10/ghfw8w.

[101] ISO, 'Mechanical vibration and shock — Evaluation of human exposure to whole-body vibration — Part 1: General requirements', International Organization for Standardization, Geneva, ISO Standard 2631-1, 1997.

[102] J. Bos and W. Bles, 'Modelling motion sickness and subjective vertical mismatch detailed for vertical motions', *Brain Research Bulletin*, vol. 47, no. 5, pp. 537–542, Nov. 1998. DOI: 10/b9spsq.

[103] R. Telban and F. Cardullo, 'An integrated model of human motion perception with visual-vestibular interaction', in *AIAA Modeling and Simulation Technologies Conference and Exhibit*, Montreal,Canada: American Institute of Aeronautics and Astronautics, 6th Aug. 2001. DOI: 10/ghdccm.

[104] L. Zuo and S. Nayfeh, 'Low order continuous-time filters for approximation of the ISO 2631-1 human vibration sensitivity weightings', *Journal of Sound and Vibration*, vol. 265, no. 2, pp. 459–465, Aug. 2003. DOI: 10/dgpmtz.

[105] A. Lawther and M. J. Griffin, 'Prediction of the incidence of motion sickness from the magnitude, frequency, and duration of vertical oscillation', *The Journal of the Acoustical Society of America*, vol. 82, no. 3, pp. 957–966, Sep. 1987. DOI: 10/cw29cs.

[106] C. Braccesi and F. Cianetti, 'Motion sickness. Part I: Development of a model for predicting motion sickness incidence', *International Journal of Human Factors Modelling and Simulation*, vol. 2, no. 3, p. 163, 2011. DOI: 10/fx2m69.

[107] J. F. Golding, D. Phil, M. I. Finch and J. R. R. Stott, 'Frequency effect of 0.35-1.0Hz horizontal translational oscillation on motion sickness and the somatogravic illusion', *Aviation, Space, and Environmental Medicine*, vol. 68, no. 5, pp. 396–402, 1997.

[108] N. Kamiji, Y. Kurata, T. Wada and S. Doi, 'Modeling and validation of carsickness mechanism', in *SICE Annual Conference 2007*, Takamatsu, Japan: IEEE, Sep. 2007, pp. 1138–1143, ISBN: 978-4-907764-27-2. DOI: 10/fmvp69.

[109] D. C. Zikovitz and L. R. Harris, 'Head tilt during driving', *Ergonomics*, vol. 42, no. 5, pp. 740–746, May 1999. DOI: 10/fpcb35.

[110] T. Wada, S. Fujisawa and S. Doi, 'Analysis of driver's head tilt using a mathematical model of motion sickness', *International Journal of Industrial Ergonomics*, vol. 63, pp. 89–97, Jan. 2018. DOI: 10/ggp87n.

[111] T. Sugiura, T. Wada, T. Nagata, K. Sakai and Y. Sato, 'Analysing Effect of Vehicle Lean Using Cybernetic Model of Motion Sickness', *IFAC-PapersOnLine*, vol. 52, no. 19, pp. 311–316, 2019. DOI: 10/ggp88q.

[112] G. Bertolini, M. A. Durmaz, K. Ferrari, A. Küffer, C. Lambert and D. Straumann, 'Determinants of Motion Sickness in Tilting Trains: Coriolis/Cross-Coupling Stimuli and Tilt Delay', *Frontiers in Neurology*, vol. 8, p. 195, 15th May 2017. DOI: 10/ggqc6r.

[113] P. DiZio, J. Ekchian, J. Kaplan, J. Ventura, W. Graves, M. Giovanardi, Z. Anderson and J. R. Lackner, 'An Active Suspension System for Mitigating Motion Sickness and Enabling Reading in a Car', *Aerospace Medicine and Human Performance*, vol. 89, no. 9, pp. 822–829, 1st Sep. 2018. DOI: 10/ghdcch.

[114] D. Bohrmann and K. Bengler, 'Reclined Posture for Enabling Autonomous Driving', in *Human Systems Engineering and Design II*, ser. Advances in Intelligent Systems and Computing, T. Ahram, W. Karwowski, S. Pickl and R. Taiar, Eds., vol. 1026, Cham: Springer International Publishing, 2020, pp. 169–175, ISBN: 978-3-030-27927-1. DOI: 10.1007/978-3-030-27928-8_26.

[115] O. X. Kuiper, J. E. Bos and C. Diels, 'Looking forward: In-vehicle auxiliary display positioning affects carsickness', *Applied Ergonomics*, vol. 68, pp. 169–175, Apr. 2018. DOI: 10/ggp85x.

[116] S. Salter, C. Diels, P. Herriotts, S. Kanarachos and D. Thake, 'Motion sickness in automated vehicles with forward and rearward facing seating orientations', *Applied Ergonomics*, vol. 78, pp. 54–61, Jul. 2019. DOI: 10/ggp868.

[117] J. Karjanto, N. Md. Yusof, C. Wang, J. Terken, F. Delbressine and M. Rauterberg, 'The effect of peripheral visual feedforward system in enhancing situation awareness and mitigating motion sickness in fully automated driving', *Transportation Research Part F: Traffic Psychology and Behaviour*, vol. 58, pp. 678–692, Oct. 2018. DOI: 10/gfhfts.

[118] A. Meschtscherjakov, S. Strumegger and S. Trösterer, 'Bubble Margin: Motion Sickness Prevention While Reading on Smartphones in Vehicles', in *Human-Computer Interaction – INTERACT 2019*, ser. Lecture Notes in Computer Science, D. Lamas, F. Loizides, L. Nacke, H. Petrie, M. Winckler and P. Zaphiris, Eds., vol. 11747, Cham: Springer International Publishing, 2019, pp. 660–677, ISBN: 978-3-030-29383-3. DOI: 10.1007/978-3-030-29384-0_39.

[119] D. Damböck, T. Weißgerber, M. Kienle and K. Bengler, 'Evaluation of a contact analog head-up display for highly automated driving', 2012.

[120] P. Feenstra, J. Bos and R. van Gent, 'A visual display enhancing comfort by counteracting airsickness', *Displays*, vol. 32, no. 4, pp. 194–200, Oct. 2011. DOI: 10/fnp6k9.

[121] S. A. Saruchi, M. H. Mohammed Ariff, H. Zamzuri, N. H. Amer, N. Wahid, N. Hassan and K. A. A. Kassim, 'Novel Motion Sickness Minimization Control via Fuzzy-PID Controller for Autonomous Vehicle', *Applied Sciences*, vol. 10, no. 14, p. 4769, 10th Jul. 2020. DOI: 10/ghd79b.

[122] G. M. Hoffmann, C. J. Tomlin, M. Montemerlo and S. Thrun, 'Autonomous Automobile Trajectory Tracking for Off-Road Driving: Controller Design, Experimental Validation and Racing', in *2007 American Control Conference*, New York, NY, USA: IEEE, Jul. 2007, pp. 2296–2301, ISBN: 978-1-4244-0988-4. DOI: 10/fd7r3j.

[123] M. Sever, N. Zengin, A. Kirli and M. S. Arslan, 'Carsickness-based design and development of a controller for autonomous vehicles to improve the comfort of occupants', *Proceedings of the Institution of Mechanical Engineers, Part D: Journal of Automobile Engineering*, p. 095 440 702 094 331, 30th Jul. 2020. DOI: 10/ghf99b.

[124] Z. Htike, G. Papaioannou, E. Siampis, E. Velenis and S. Longo, 'Motion Sickness Minimisation in Autonomous Vehicles Using Optimal Control', in *Advances in Service and Industrial Robotics*, ser. Mechanisms and Machine Science, S. Zeghloul, M. A. Laribi and J. S. Sandoval Arevalo, Eds., vol. 84, Cham: Springer International Publishing, 2020, pp. 275–282, ISBN: 978-3-030-48988-5. DOI: 10.1007/978-3-030-48989-2_30.

[125] A. Chowdhury, R. Shankaran, M. Kavakli and M. M. Haque, 'Sensor Applications and Physiological Features in Drivers' Drowsiness Detection: A Review', *IEEE Sensors Journal*, vol. 18, no. 8, pp. 3055–3067, 15th Apr. 2018. DOI: 10/gdbxfj.

[126] H. Hu, Y. Zhu, Y. Zhang, Q. Zhou, Y. Feng and G. Tan, 'Comprehensive Driver State Recognition Based on Deep Learning and PERCLOS Criterion', in *2019 IEEE 19th International Conference on Communication Technology (ICCT)*, Xi'an, China: IEEE, Oct. 2019, pp. 1678–1682, ISBN: 978-1-72810-535-2. DOI: 10/ghgdqm.

[127] A. Atkielski, *Schematic representation of normal sinus rhythm showing standard wave, segments, and intervals.*

[128] G. G. Berntson, K. S. Quigley, J. F. Jang and S. T. Boysen, 'An Approach to Artifact Identification: Application to Heart Period Data', *Psychophysiology*, vol. 27, no. 5, pp. 586–598, Sep. 1990. DOI: 10/bhftdb.

[129] N. Wessel, A. Voss, H. Malberg, C. Ziehmann, H. U. Voss, A. Schirdewan, U. Meyerfeldt and J. Kurths, 'Nonlinear analysis of complex phenomena in cardiological data', *Herzschrittmachertherapie und Elektrophysiologie*, vol. 11, no. 3, pp. 159–173, 19th Oct. 2000. DOI: 10/c2pvq4.

[130] L. Citi, E. N. Brown and R. Barbieri, 'A Real-Time Automated Point-Process Method for the Detection and Correction of Erroneous and Ectopic Heartbeats', *IEEE Transactions on Biomedical Engineering*, vol. 59, no. 10, pp. 2828–2837, Oct. 2012. DOI: 10/f39wp3.

[131] L. dos Santos, J. J. Barroso, E. E. Macau and M. F. de Godoy, 'Application of an automatic adaptive filter for Heart Rate Variability analysis', *Medical Engineering & Physics*, vol. 35, no. 12, pp. 1778–1785, Dec. 2013. DOI: 10/ghdccp.

[132] T. F. o. t. E. S. o. C. t. N. A. S. Electrophysiology, 'Heart Rate Variability : Standards of Measurement, Physiological Interpretation, and Clinical Use', *Circulation*, vol. 93, no. 5, pp. 1043–1065, 1st Mar. 1996. DOI: 10/bvcx8p.

[133] M. Brennan, M. Palaniswami and P. Kamen, 'Do existing measures of Poincare plot geometry reflect nonlinear features of heart rate variability?', *IEEE Transactions on Biomedical Engineering*, vol. 48, no. 11, pp. 1342–1347, Nov. 2001. DOI: 10/ccxc62.

[134] J. Piskorski and P. Guzik, 'Geometry of the Poincaré plot of RR intervals and its asymmetry in healthy adults', *Physiological Measurement*, vol. 28, no. 3, pp. 287–300, 1st Mar. 2007. DOI: 10/cp4kkb.

[135] M.-Z. Poh, D. J. McDuff and R. W. Picard, 'Advancements in Noncontact, Multiparameter Physiological Measurements Using a Webcam', *IEEE Transactions on Biomedical Engineering*, vol. 58, no. 1, pp. 7–11, Jan. 2011. DOI: 10/bjr5hk.

[136] M.-Z. Poh, D. J. McDuff and R. W. Picard, 'Non-contact, automated cardiac pulse measurements using video imaging and blind source separation', *Optics Express*, vol. 18, no. 10, p. 10 762, 10th May 2010. DOI: 10/btzz88.

[137] P. Viola and M. J. Jones, 'Robust Real-Time Face Detection', *International Journal of Computer Vision*, vol. 57, no. 2, pp. 137–154, May 2004. DOI: 10/d3s76r.

[138] P. Comon, 'Independent component analysis, A new concept?', *Signal Processing*, vol. 36, no. 3, pp. 287–314, Apr. 1994. DOI: 10/cx6rr9.

[139] P. Comon and C. Jutten, Eds., *Handbook of Blind Source Separation: Independent Component Analysis and Applications*, 1st ed. Amsterdam ; Boston: Elsevier, 2010, 831 pp., ISBN: 978-0-12-374726-6.

[140] Y. Sun, C. Papin, V. Azorin-Peris, R. Kalawsky, S. Greenwald and S. Hu, 'Comparison of scientific CMOS camera and webcam for monitoring cardiac pulse after exercise', presented at the SPIE Optical Engineering + Applications, A. G. Tescher, Ed., San Diego, California, USA, 8th Sep. 2011, p. 813 506. DOI: 10/djb839.

[141] A. Lam and Y. Kuno, 'Robust Heart Rate Measurement from Video Using Select Random Patches', in *2015 IEEE International Conference on Computer Vision (ICCV)*, Santiago, Chile: IEEE, Dec. 2015, pp. 3640–3648, ISBN: 978-1-4673-8391-2. DOI: 10/ghdcd3.

[142] M. I. Davila, G. F. Lewis and S. W. Porges, 'The PhysioCam: Cardiac Pulse, Continuously Monitored by a Color Video Camera [1]', *Journal of Medical Devices*, vol. 10, no. 2, p. 020 951, 12th May 2016. DOI: 10/ghdcfc.

[143] Z. Guo, Z. J. Wang and Z. Shen, 'Physiological parameter monitoring of drivers based on video data and independent vector analysis', in *2014 IEEE International Conference on Acoustics, Speech and Signal Processing (ICASSP)*, Florence, Italy: IEEE, May 2014, pp. 4374–4378, ISBN: 978-1-4799-2893-4. DOI: 10/ghdcdt.

[144] C. Sagonas, G. Tzimiropoulos, S. Zafeiriou and M. Pantic, '300 Faces in-the-Wild Challenge: The First Facial Landmark Localization Challenge', in *2013 IEEE International Conference on Computer Vision Workshops*, Sydney, Australia: IEEE, Dec. 2013, pp. 397–403, ISBN: 978-1-4799-3022-7. DOI: 10/ghgjcc.

[145] T. Kim, T. Eltoft and T.-W. Lee, 'Independent Vector Analysis: An Extension of ICA to Multivariate Components', in *Independent Component Analysis and Blind Signal Separation*, J. Rosca, D. Erdogmus, J. C. Príncipe and S. Haykin, Eds., red. by D. Hutchison, T. Kanade, J. Kittler, J. M. Kleinberg, F. Mattern, J. C. Mitchell, M. Naor, O. Nierstrasz, C. Pandu Rangan, B. Steffen, M. Sudan, D. Terzopoulos, D. Tygar, M. Y. Vardi and G. Weikum, vol. 3889, Berlin, Heidelberg: Springer Berlin Heidelberg, 2006, pp. 165–172, ISBN: 978-3-540-32630-4. DOI: 10.1007/11679363_21.

[146] T. Taniguchi, N. Ono, A. Kawamura and S. Sagayama, 'An auxiliary-function approach to online independent vector analysis for real-time blind source separation', in *2014 4th Joint Workshop on Hands-Free Speech Communication and Microphone Arrays (HSCMA)*, Villers-les-Nancy, France: IEEE, May 2014, pp. 107–111, ISBN: 978-1-4799-3109-5. DOI: 10/ghdccj.

[147] S. Zafeiriou, G. G. Chrysos, A. Roussos, E. Ververas, J. Deng and G. Trigeorgis, 'The 3D Menpo Facial Landmark Tracking Challenge', in *2017 IEEE International Conference on Computer Vision Workshops (ICCVW)*, Venice, Italy: IEEE, Oct. 2017, pp. 2503–2511, ISBN: 978-1-5386-1034-3. DOI: 10/ggssn4.

[148] P. Padeleris, X. Zabulis and A. A. Argyros, 'Head pose estimation on depth data based on Particle Swarm Optimization', in *2012 IEEE Computer Society Conference on Computer Vision and Pattern Recognition Workshops*, Providence, RI, USA: IEEE, Jun. 2012, pp. 42–49, ISBN: 978-1-4673-1612-5. DOI: 10/ggnbbr.

[149] Y. Gao, A. Gray, J. V. Frasch, T. Lin, E. Tseng, J. K. Hedrick and F. Borrelli, 'Spatial Predictive Control for Agile Semi-Autonomous Ground Vehicles', in *Proceedings of the 11th International Symposium on Advanced Vehicle Control*, 2012.

[150] M. M. Graf Plessen and A. Bemporad, 'Reference trajectory planning under constraints and path tracking using linear time-varying model predictive control for agricultural machines', *Biosystems Engineering*, vol. 153, pp. 28–41, Jan. 2017. DOI: 10/f9p9rs.

[151] M. G. Plessen, P. F. Lima, J. Martensson, A. Bemporad and B. Wahlberg, 'Trajectory planning under vehicle dimension constraints using sequential linear programming', in *2017 IEEE 20th International Conference on Intelligent Transportation Systems (ITSC)*, Yokohama: IEEE, Oct. 2017, pp. 1–6, ISBN: 978-1-5386-1526-3. DOI: 10/gd8wfw.

[152] M. Graf Plessen, D. Bernardini, H. Esen and A. Bemporad, 'Spatial-Based Predictive Control and Geometric Corridor Planning for Adaptive Cruise Control Coupled With Obstacle Avoidance', *IEEE Transactions on Control Systems Technology*, vol. 26, no. 1, pp. 38–50, Jan. 2018. DOI: 10/gcqc22.

[153] F. H. Speckhart and E. Harrison, 'The Design of a Shock Absorber to Improve Ride Comfort by Reducing Jerk', presented at the Mid-Year Meeting, 1st Feb. 1968, p. 680 472. DOI: 10/fvxzjt.

[154] J. Baumann, D. D. Torkzadeh, A. Ramstein, U. Kiencke and T. Schlegl, 'Model-Based Predictive Anti-Jerk Control', *IFAC Proceedings Volumes*, vol. 37, no. 22, pp. 53–58, Apr. 2004. DOI: 10/ghgqdr.

[155] C. Certosini, L. Papini, R. Capitani and C. Annicchiarico, 'Preliminary study for motion sickness reduction in autonomous vehicles: An MPC approach', *Procedia Structural Integrity*, vol. 24, pp. 127–136, 2019. DOI: 10/ggqc6v.

[156] T. Novi, 'A control system framework for autonomous vehicles at the limits of handling', Ph.D. thesis, Università degli Studi di Firenze, Florence, 2019, 122 pp.

[157] C. Certosini, R. Capitani and C. Annicchiarico. 'Optimal speed profile on a given road for motion sickness reduction'. arXiv: 2010.05701 [cs, eess]. (12th Oct. 2020), [Online]. Available: http://arxiv.org/abs/2010.05701 (visited on 13/10/2020).

[158] P. Varaiya, 'Smart cars on smart roads: Problems of control', *IEEE Transactions on Automatic Control*, vol. 38, no. 2, pp. 195–207, Feb. 1993. DOI: 10/dsmm4m.

[159] C. Katrakazas, M. Quddus, W.-H. Chen and L. Deka, 'Real-time motion planning methods for autonomous on-road driving: State-of-the-art and future research directions', *Transportation Research Part C: Emerging Technologies*, vol. 60, pp. 416–442, Nov. 2015. DOI: 10/f7z6wb.

[160] I. Bae, Jaeyoung Moon, Hyunbin Park, J. H. Kim and S. Kim, 'Path generation and tracking based on a Bezier curve for a steering rate controller of autonomous vehicles', in *16th International IEEE Conference on Intelligent Transportation Systems (ITSC 2013)*, The Hague, Netherlands: IEEE, Oct. 2013, pp. 436–441, ISBN: 978-1-4799-2914-6. DOI: 10/ghd8b4.

[161] A. Heilmeier, A. Wischnewski, L. Hermansdorfer, J. Betz, M. Lienkamp and B. Lohmann, 'Minimum curvature trajectory planning and control for an autonomous race car', *Vehicle System Dynamics*, vol. 58, no. 10, pp. 1497–1527, 2nd Oct. 2020. DOI: 10/ggjqvx.

[162] X. Li, Z. Sun, Q. Zhu and D. Liu, 'A unified approach to local trajectory planning and control for autonomous driving along a reference path', in *2014 IEEE International Conference on Mechatronics and Automation*, Tianjin, China: IEEE, Aug. 2014, pp. 1716–1721, ISBN: 978-1-4799-3979-4. DOI: 10/ghd8cb.

[163] A. Liniger, A. Domahidi and M. Morari, 'Optimization-based autonomous racing of 1:43 scale RC cars', *Optimal Control Applications and Methods*, vol. 36, no. 5, pp. 628–647, Sep. 2015. DOI: 10/f7xvzv.

[164] A. Liniger and J. Lygeros, 'Real-Time Control for Autonomous Racing Based on Viability Theory', *IEEE Transactions on Control Systems Technology*, vol. 27, no. 2, pp. 464–478, Mar. 2019. DOI: 10/ghdcdx.

[165] F. Christ, A. Wischnewski, A. Heilmeier and B. Lohmann, 'Time-optimal trajectory planning for a race car considering variable tyre-road friction coefficients', *Vehicle System Dynamics*, pp. 1–25, 22nd Dec. 2019. DOI: 10/ggjqwg.

[166] J. R. Anderson and B. Ayalew, 'Modelling minimum-time manoeuvering with global optimisation of local receding horizon control', *Vehicle System Dynamics*, vol. 56, no. 10, pp. 1508–1531, 3rd Oct. 2018. DOI: 10/ghp2rw.

Acronyms

AD Autonomous Driving. v, 1, 2, 14, 16, 43, 56

ADAS Advanced driver-Assistance Systems. 56, 58

ANN Artificial Neural Networks. 24, 25

EDA Electro-Dermal Activity. 7, 19

EOG Electro-OculoGraphy. 19

EU European Union. 1

GIA Gravito-Inertial Acceleration. 9, 14, 15, 26

GVS Galvanic Vestibular Stimulation. 9

HMI Human-Machine Interface. 30

HRV Heart Rate Variability. 3, 7, 19, 20, 24, 25, 27, 57, 58

HUD Head-Up Display. 16

IBI Inter-Beat Intervals. 20, 24, 25

ICA Indipendent Component Analysis. 24

IVA Indipendent Vector Analysis. 24, 25

LQR Linear Quadratic Regulator. 17

MPC Model Predictive Control. v, 35, 46, 47, 50

MS Motion Sickness. v, 2, 3, 5, 7–10, 12–17, 19, 20, 25–27, 29–31, 33–37, 39, 42, 43, 45–47, 49, 50, 52, 55–58

MSAQ Motion Sickness Assessment Questionnaire. 8

MSDV Motion Sickness Dose Value. 11, 17

MSHQ Motion Sickness History Questionnaire. 8

MSI Motion Sickness Incidence. v, xi, 3, 5, 6, 10–16, 19, 25–27, 29, 31, 32, 34–37, 39, 42, 43, 45–47, 49–52, 55–58

MSQ Pensacola Motion Sickness Questionnaire. 8

MSSQ Motion Sickness Susceptibility Questionnaire. 8

MSSQR Motion Sickness Susceptibility Questionnaire Revised. 8

NMPC Non-linear Model Predictive Control. 3, 30, 33, 46, 55, 57

PSD Power Spectral Density. 20, 39, 52, 55

ROI Region Of Interest. 24

SSQ Simulator Sickness Questionnaire. 8

VRSQ Virtual-Reality Sickness Questionnaire. 8